Inorg. Chem. **2003**, *42*, 4828–4841

Formation of Two Diverse Classes of Poly(amino-alkoxide) Chelates and Their Mononuclear and Polynuclear Lanthanide(III) Complexes

Marlon K. Thompson,[†] Alan J. Lough,[‡] Andrew J. P. White,[§] David J. Williams,[§] and Ishenkumba A. Kahwa*,[†]

Chemistry Department, University of the West Indies, Mona Campus, Kingston 7, Jamaica, West Indies, Department of Chemistry, University of Toronto, 80 St. George Street, Toronto, Ontario M5S 3H6, Canada, and Chemistry Department, Imperial College London, South Kensington, London SW7 2AY, U.K.

Received February 25, 2002

Factors that influence aggregation of lanthanide(III) (Ln^{III}) ions to form polynuclear complexes were studied utilizing 1-aziridineethanol as a versatile source of macrocyclic and acyclic chelates. The facile ring-opening cyclo-oligomerization of 1-aziridineethanol leads to the formation of a series of polyaza cyclic oligomers (series A). In the presence of ethylenediamine, a competing N-alkylation reaction occurs to produce a new class of acyclic ligands (series B). The cyclo-oligomerization of four 1-aziridineethanol units is the most favorable process, leading to the formation of the 12-membered cyclen-type macrocycle, $H_4\mathbf{L^1}$ (1,4,7,10-tetrakis(2-hydroxyethyl)-1,4,7,10-tetraazacyclododecane). Ring-opening cyclo-oligomerization of 1-aziridineethanol in the presence of Ln^{III} ions produces self-assembled mononuclear, tetranuclear, and pentanuclear compounds of $H_4\mathbf{L^1}$. In the presence of ethylenediamine, oligomerization of 1-aziridineethanol results in a dinuclear complex of an acyclic poly(amino-alkoxide) $H_2\mathbf{L^2}$. The coordinative unsaturation of (i) the alkoxy sites of $[H_x\mathbf{L^1}]^{x-4}$ (where $x < 4$) and (ii) Ln^{III} ions in coordination numbers less than nine are critical factors in the formation of the polynuclear Ln^{III} complexes. The identities of mononuclear, dinuclear, tetranuclear, and pentanuclear complexes herein discussed were established by X-ray crystallography.

Introduction

Mononuclear complexes of rare earth ions, particularly the lanthanides, continue to attract considerable attention because of their electronic and nuclear properties which are of great interest to contrast enhancement in magnetic resonance imaging (MRI) (Gd^{III}),[1] luminescent bio-probes[2,3] (Eu^{III}, Tb^{III}, and Yb^{III}), radiopharmaceuticals (^{90}Y and ^{153}Sm),[4] and, more recently, luminescent computational logic gates (Eu^{III} and Tb^{III}).[5] Sequestration and subsequent transportation of rare earth ions as kinetically and/or thermodynamically stable complexes in aqueous environments is a crucial requirement in many of these applications. Therefore, there is sustained interest toward the design of multidentate ligands capable of forming stable Ln^{III} complexes for solution applications.[1−7]

A promising ligand design is the manipulation of the ring-opening reaction of N-substituted aziridines as a route to

* Corresponding author. E-mail: ikahwa@uwimona.edu.jm. Phone: (876) 927-1910. Fax: (876) 876-1834.
[†] University of the West Indies.
[‡] University of Toronto.
[§] Imperial College.

(1) (a) Aime, S.; Botta, M.; Fasano, M.; Terreno, E. *Chem. Soc. Rev.* **1998**, *27*, 19. (b) Laufer, R. B. *Chem. Rev.* **1987**, *87*, 901. (c) Caravan, P.; Ellison, J. J.; McMurry, T. J.; Laufer, R. B. *Chem. Rev.* **1999**, *99*, 2293. (d) Botta, M. *Eur. J. Inorg. Chem.* **2000**, 399.
(2) Good reviews on these subjects can be found in: (a) *Topics in Fluorescence Spectroscopy*; Lakowicz, J. R., Ed.; Plenum Press: New York, 1991−1994; Vols. 1−4. (b) Lakowicz, J. R. *Principles of Fluorescence Spectroscopy*, 2nd ed.; Kluwer Academic/Plenum Publishers: New York, 1999. (c) *Fluorescence Microscopy and Fluorescent Probes*; Slavík, J., Ed.; Plenum Press: New York, 1996.
(3) (a) Werts, M. H. V.; Verhoeven, J. W.; Hofstraat, J. W. *J. Chem. Soc., Perkin Trans. 2* **2000**, 433. (b) Beeby, A. B.; Dickins, R. S.; Faulkner, S.; Parker, D.; Williams, J. A. G. *Chem. Commun*. **1997**, 1401.
(4) (a) Parker, D. *Chem. Soc. Rev*. **1990**, *19*, 271. (b) Jang, H. Y.; Blanco, M.; Dasgupta, S.; Keire, D. A.; Shively, J. E.; Goddard, W. A., III. *J. Am. Chem. Soc*. **1999**, *121*, 6142. (c) Heeg, M. J.; Jurisson, S. S. *Acc. Chem. Res*. **1999**, *32*, 1053.
(5) Gunnlaugsson, T.; Mac Dónail, D. A.; Parker, D. *Chem. Commun*. **2000**, 93.
(6) Piguet, C.; Bünzli, J.-C. G. *Chem. Soc. Rev.* **1999**, *28*, 347.
(7) (a) Guerriero, P.; Tamburini, S.; Vigato, P. A. *Coord. Chem. Rev*. **1995**, *139*, 17. (b) Parker, D.; Williams, J. A. G. *J. Chem. Soc., Dalton Trans*. **1996**, 3613. (c) Arnaud-Neu, F. *Chem. Soc. Rev*. **1994**, *23*, 235. (d) Alexander, V. *Chem. Rev*. **1995**, *95*, 273.

10.1021/ic020154a CCC: $25.00
Published on Web 07/16/2003

Chart 1. Some Cyclen-type Macrocycles of Interest

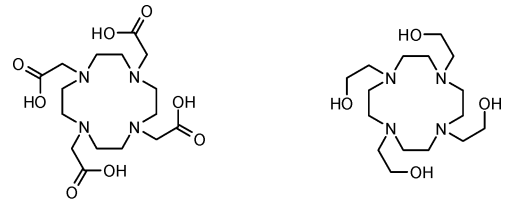

DOTA H_4L^1

cyclic and acyclic compounds.[8−11] Yb^{III} is known to catalyze the ring-opening reaction of N-substituted aziridines with primary amines to produce relatively simple substituted 1,2-diamines,[9] and the Sc^{III}-mediated ring-opening of aziridine carboxylates was also reported recently.[10] However, while N-substituted aziridines are a useful route to acyclic chelates,[11] their chemistry is also utilized to produce cyclic oligomers. Previous studies[8,12−14] have shown that the ring-opening cyclo-oligomerization of N-substituted aziridines produces polyaza cyclic compounds: cyclic tetramers are generally the major products of these reactions. Therefore, N-substituted aziridines represent a potential direct route to cyclen-type chelates with a rich array of pendant arm functionalities, depending on the nature of the N-substituent. The critical role of cyclen-based macrocylic chelates in lanthanide coordination chemistry is well documented[1,6,7] along with applications in several fields. For example, three Gd^{III} complexes of cyclen-based chelates, e.g., DOTA (Chart 1), are currently in clinical use as contrast agents for MRI diagnosis while many others are in development.[1c]

Furthermore, the chemistry of Ln^{III} ions with $H_4\mathbf{L^1}$ (Chart 1), the major product in the cyclo-oligomerization of aziridineethanol,[13] has attracted considerable interest in biomedical studies,[15−21] particularly with applications as artificial ribonucleases, and is of interest in antisense applications.[22] However, the traditional multistep synthesis[23−25] of $H_4\mathbf{L^1}$, as for most cyclen-based chelates that are in clinical MRI/radiotherapy/radioscintigraphic use or trials,[1] can be both long and expensive depending on the starting step and material.[26] Hence, the ring-opening amination reactions of N-substituted aziridines, as a facile route to cyclen-based chelates, is quite appealing.

Unlike their mononuclear counterparts, the potential of polynuclear Ln^{III} complexes for practical applications remains untapped. Although oxo-bridged polynuclear f−f complexes have been investigated to improve the efficiency of paramagnetic MRI contrast agents[27] and luminescent probes,[28,29] the potential of Ln−Ln interactions leading to enhanced properties (which can be tuned) has been underutilized. This is partly because the rational design and synthesis of polynuclear Ln^{III} complexes with specific electronic and magnetic properties (desired for MRI, luminescent, and catalytic applications) has proven to be an immense challenge.[30] A reason for this is the fact that the lanthanides display large and variable coordination numbers (6−12)[31] which are difficult to predict because the hard Ln^{III} ions tend to complete their coordination sphere by binding small molecules and anions (e.g., water, halide, hydroxide, etc.).[6] Also, several coordination polyhedra, having small energy differences, are possible for each coordination number, and the geometries around the metal center are often irregular and disordered. This imposes a difficulty in designing receptors which induce a specific geometry around the metal center. Hence, the "rational design" of polynuclear Ln^{III} complexes with specific properties is currently an inexact science, and exploratory syntheses, with the hope of discovering new materials with useful properties, has been a common alternative.[32]

Despite these synthetic challenges, the aggregation of Ln^{III} ions to form oxo-bridged clusters remains one of the stimulating frontiers in research chemistry.[33] Cluster chemistry is generally viewed as the bridge connecting molecular

(8) (a) Dermer, O. C.; Ham, G. E. *Ethylenimine and other aziridines; chemistry and applications*; Academic Press: New York, 1969. (b) Ham, G. E. In *Polymeric Amines and Ammonium Salts*; Goetals, E. J., Ed.; Pergamon: New York, 1980.
(9) Meguro, M.; Yamamaoto, Y. *Heterocycles* **1996**, *43*, 2473.
(10) Bennani, Y. L.; Zhu, G.-D.; Freeman, J. C. *Synlett.* **1998**, *7*, 754.
(11) Lorenz, I.-P.; von Beckerath, S.; Nöth, H. *Eur. J. Inorg. Chem*. **1998**, 645.
(12) Cornier, S. P.; Wymore, C. E. U.S. Patent 3 828 023, 1974.
(13) Ham, G. E.; Krause, R. L. U.S. Patent 4 093 615, 1978.
(14) Vasilevskis, J.; Varadarajan, J.; Garrity, M.; Fellmann, D. J.; Messerle, L.; Amarasinghe, G. U.S. Patent 6 048 979, 2000.
(15) Morrow, J. R.; Chin, K. O. A. *Inorg. Chem*. **1993**, *32*, 3357.
(16) Chin, K. O. A.; Morrow, J. R. *Inorg. Chem*. **1994**, *33*, 5036.
(17) Morrow, J. R.; Aures, K.; Epstein, D. *J. Chem. Soc., Chem. Commun*. **1995**, 2431.
(18) Baker, B. F.; Khalili, H.; Wei, N.; Morrow, J. R. *J. Am. Chem. Soc*. **1997**, *119*, 8749.
(19) Chappell, L. L.; Voss, D. A. V.; Horrocks, W. D., Jr.; Morrow, J. R. *Inorg. Chem*. **1998**, *37*, 3989.
(20) Baker, B. F.; Lot, S. S.; Kringel, J.; Cheng-Flournoy, S.; Villiet, P.; Sasmor, H. M.; Siwkowski, A. M.; Chappell, L. L.; Morrow, J. R. *Nucleic Acids Res*. **1999**, *27*, 1547.
(21) Epstein, D. M.; Chappell, L. L.; Khalili, H.; Supkowski, R. M.; Horrocks, W. D., Jr.; Morrow, J. R. *Inorg. Chem*. **2000**, *39*, 2130.
(22) Trawick, B. N.; Daniher, A. T.; Bashkin, J. K. *Chem. Rev*. **1998**, *98*, 939.
(23) Dhillon, R.; Lincoln, S. F.; Madbak, S.; Stephens, A. K. W.; Wainwright, K. P.; Whitbread, S. L. *Inorg. Chem*. **2000**, *39*, 1855 and references therein.
(24) Whitbread, S. L.; Valente, P.; Buntine, M. A.; Clements, P.; Lincoln, S. F.; Wainwright, K. P. J. *Am. Chem. Soc*. **1998**, *120*, 2862.
(25) (a) Buøen, S.; Dale, J.; Groth, P.; Krane, J. *J. Chem. Soc., Chem. Commun*. **1982**, 1172. (b) Groth, P. *Acta Chem. Scand., Ser. B* **1983**, *37*, 71. (c) Custelcean, R.; Vlassa, M.; Jackson, J. E. *Angew. Chem., Int. Ed*. **2000**, *39*, 3299.
(26) Prices of cyclen, ethylene oxide, and azidineethanol differ considerably depending on the supplier, but aziridineethanol is generally a cheap single source for $H_4\mathbf{L^1}$.
(27) (a) Toth, E.; Helm, L.; Merbach, A. E.; Hedinger, R.; Hegetschweiler, K.; Janossy, A. *Inorg. Chem.* **1998**, *37*, 4104. (b) Powell, D. H.; Ni Dhubhghaill, O. M.; Pubanz, D.; Helm, L.; Lebedev, Y. S.; Schlaepfer, W.; Merbach, A. E. *J. Am. Chem. Soc*. **1996**, *118*, 9333.
(28) Bünzli, J.-C. G. In *Lanthanide Probes in Life, Medical, and Environmental Sciences*; Choppin, G. R., Bünzli, J.-C. G., Eds.; Elsevier: Amsterdam, The Netherlands, 1989; Chapter 7.
(29) Sabbatini, N.; Guardigli, M.; Lehn, J.-M. *Coord. Chem. Rev*. **1993**, *123*, 201.
(30) Anwander, R. *Angew. Chem., Int. Ed*. **1998**, *37*, 599.
(31) Sinha, S. P. *Struct. Bonding (Berlin)* **1974**, *25*, 69.
(32) Hong, S.-T.; Hoistad, L. M.; Corbett, J. D. *Inorg. Chem*. **2000**, *39*, 98.
(33) (a) Setyawati, I. A.; Liu, S.; Rettig, S. J.; Orvig, C. *Inorg. Chem*. **2000**, *39*, 496. (b) Wang, R.; Zheng, Z.; Jin, T.; Staples, R. J. *Angew. Chem., Int. Ed.*. **1999**, *38*, 1813. (c) Burgstein, M. R.; Roesky, P. W. *Angew. Chem., Intl. Ed.* **2000**, *39*, 549. (d) Wang, R.; Carducci, M. D.; Zheng, A. *Inorg. Chem*. **2000**, *39*, 1836. (e) Ma, B.-Q.; Zhang, D.-S.; Gao, S.; Jin, T.-Z.; Yan, C.-H.; Xu, G.-X. *Angew. Chem., Intl. Ed*. **2000**, *39*, 3644. (f) Wang, R.; Liu, H.; Carducci, M. D.; Jin. T.; Zheng, C.; Zheng, Z. *Inorg. Chem*. **2001**, *40*, 2743.

and solid state chemistry, and inorganic clusters, in particular, continue to attract considerable attention because they are useful tools for understanding the size-dependent physical properties of electronic materials.[34,35] While the rational design of high symmetry coordination clusters has been achieved for transition metals,[36] general synthetic guidelines have not yet evolved for the lanthanides. We have therefore embarked on a research initiative to investigate the factors which influence the assembly of Ln^{III} ions into clusters of unique shape and composition.[37,38]

To this end, we are currently exploring different classes of poly(amino-alkoxides) as a route to novel multidentate chelates with differing architecture and denticity, the ultimate aim being to form novel Ln^{III} aggregates featuring potentially interesting physical properties. Central to our ligand design are the successive N-alkylations of polyamines and cyclo-oligomerizations involving N-substituted aziridine functionalities to produce Ln^{III} chelates. For example, with N-alkoxy aziridines, such alkylations can potentially yield polyanionic cyclic and acyclic poly(amino-alkoxides)[8,13] suitable for synthesizing novel thermodynamically and kinetically stable Ln^{III} complexes. Polymetallic aggregates with potential for cooperative chemical or electronic activity among proximal Ln^{III} cations are of particular interest.[37−39] For example, the mononuclear Ln^{III} complexes of $H_4\mathbf{L^1}$ catalyze the hydrolysis of phosphodiester bridges of RNA at impressive rates.[15−21] However, it has been proposed that, for these reactions, the catalytically active species in solution is generally the oxo-bridged dinuclear complex.[40] The catalytic activity of polynuclear complexes of $H_4\mathbf{L^1}$ is yet to be assessed, possibly due to the challenges in synthesizing these molecules.

Herein we report the preparation of a series of cyclic (series A) and novel acyclic (series B) poly(amino-alkoxides) (Scheme 1). The formation and elegant crystal structures of a self-assembled praseodymium(III) dimer of $H_2\mathbf{L^2}$ as well as Ln^{III} mononuclear, tetranuclear, and pentanuclear complexes of $H_4\mathbf{L^1}$ and its deprotonated derivatives are also presented. The critical role of coordinative unsaturation in the assembly of the lanthanide(III) clusters will be discussed.

Experimental Section

Spectral and Quantitative Analyses. Fast atom bombardment (FAB) and liquid secondary ion mass spectrometry (LSIMS) mass spectra (in *m*-nitrobenzyl alcohol matrix) were obtained using a Concept mass spectrometer at Cambridge University or a VG Masslab Trio-2 at the University of Miami. Isotopic abundance patterns were calculated using the program that is freely available at the Sheffield University website: http://www.shef.ac.uk/chemistry/chemputer/isotopes.html.

Carbon−hydrogen−nitrogen analyses were done at MEDAC Ltd., Surrey, U.K. Infrared spectra were obtained from either a Perkin-Elmer 1000S or 1600S FT-IR spectrometer with samples prepared in KBr disks.

The luminescence and excitation spectra were recorded using a FluoroMax-2 spectrofluorometer with samples sealed in glass tubes. Luminescence decay curves were acquired using either a ND6000 dye laser pumped by a Continuum Powerlite 8000 Nd:YAG laser or a Photon Technology International PL201 dye laser pumped by a PL2300 nitrogen laser as described previously.[39b] Selective excitation for Eu^{III} ($^5D_0$) was achieved using a Rhodamine6G dye tuned at 579 nm.

Materials. Lanthanide(III) nitrates and perchlorates were obtained by neutralizing the respective lanthanide oxides (Aldrich; 99.99% purity) with concentrated nitric acid and perchloric acid, respectively, and then evaporating the liquid to dryness. *Warning: Metal perchlorates are very unstable and potentially explosive materials that must be handled with much care and in small quantities.* 1-Aziridineethanol was obtained from Aldrich in 97% purity (stabilized by dissolved 1−3% sodium hydroxide). Ethylenediamine was obtained from BDH in 99% purity.

Preparation of Compounds. Cyclic Oligomers (Series A). A series of cyclic oligomers of formula $[CH_2CH_2NCH_2CH_2OH]_n$ ($n = 2-13$) (series A) were synthesized by refluxing 1-aziridineethanol (1 mmol) in 100 cm^3 of anhydrous ethanol for 24 h. Rotary evaporation of ethanol resulted in a viscous yellow oil (**1**). FAB MS: $m/z = 87 + 87m$ [$m = 1-13$]; the macrocycles are stabilized by sodium(I) in the FAB MS environment.

Cyclic Oligomers (Series A) and Acyclic Oligomers (Series B). A series of cyclic (series A) and acyclic (series B) poly(amino-alkoxide) oligomers were synthesized by refluxing 1-aziridineethanol (56.2 mmol) and ethylenediamine (28.1 mmol) in anhydrous acetonitrile. Rotary evaporation of acetonitrile resulted in a viscous yellow oil (**2**). FAB MS is dominated by series B: $m/z = 235 + 87m$ [$m = 0-18$].

$[Ln(H_4\mathbf{L^1})(H_2O)][Ln(NO_3)_6]\cdot 0.5CH_3CH_2OH$ (3, Ln = La, Pr). 1-Aziridineethanol (2.0 mmol) was added dropwise to $Ln(NO_3)_3\cdot nH_2O$ (1.0 mmol) in 200 cm^3 of warm anhydrous ethanol, and the resulting solution (of pH 5) was placed on a warm hot plate. The resulting precipitate was filtered off and the filtrate evaporated slowly resulting in deposition of cubic crystals the analyses of which corresponded to the stoichiometry $[Ln(H_4\mathbf{L^1})(H_2O)][Ln(NO_3)_6]\cdot 0.5CH_3CH_2OH$ (ca. 8% yield based on Ln). Anal. Calcd (%) for Ln = La: C, 19.6; H, 3.9; N, 13.5. Found: C, 19.59; H, 4.12; N, 13.22. Anal. Calcd (%) for Ln = Pr: C, 19.6; H, 3.9; N, 13.4. Found: C, 19.29; H, 4.07; N, 13.34. FAB MS: $m/z = 487$ [Pr-$(H_2\mathbf{L^1})]^+$. IR (KBr disk; cm^{-1}): 1336, 1446 (bidentate NO_3^-).

$[Ln(H_4\mathbf{L^1})(H_2O)]\cdot[ClO_4]_3\cdot X$ (X = Solvent; Ln = Eu−Tb) (4). $Ln(ClO_4)_3\cdot nH_2O$ (1.0 mmol) in 45 cm^3 of 3:1 CH_3CN/CH_3OH was added dropwise over 2 h to a refluxing solution of 1-aziridineethanol (2.0 mmol) in 100 cm^3 of 3:1 CH_3CN/CH_3OH resulting in deposition of a white precipitate. Reflux was continued for 1 h, and then, ethylenediamine (1.0 mmol) was added and the solution refluxed for 3 days. The mixture was filtered and the filtrate (of pH 6) evaporated slowly to obtain colorless crystals of the product in 10−15% yield. Anal. Calcd (%) for $([Gd(H_4\mathbf{L^1})(H_2O)]\cdot(ClO_4)_3\cdot 0.4CH_3CN$ (**4**, Ln = Gd) ($C_{16.8}Cl_3H_{39.6}N_{4.4}O_{17}Gd$): C, 24.1;

(34) Reviews: (a) Bönnemann, H.; Richards, R. M. *Eur. J. Inorg. Chem.* **2001**, 2455. (b) Schmid, G.; Bäumle, M.; Geerkens, M.; Heim, I.; Osemann, C.; Sawitowski, T. *Chem. Soc. Rev.* **1999**, *28*, 179.

(35) (a) *Clusters and Colloids: From Theory to Applications*; Schmidt, G., Ed.; VCH: Weinheim, 1994. (b) *Physics and Chemistry of Metal Cluster Compounds*; de Jongh, L. J., Ed.; Kluwer: Dordrecht, 1994.

(36) Caulder, D. L.; Raymond, K. N. *J. Chem. Soc., Dalton Trans.* **1999**, 1185.

(37) Thompson, M. K.; Kahwa, I. A.; Votchkov, M. *Inorg. Chem.* **2001**, *40*, 4332.

(38) Singh-Wilmot, M. A.; Kahwa, I. A.; White, A. J. P.; Williams, D. J. Manuscript in preparation.

(39) (a) Matthews, K. D.; Kahwa, I. A.; Williams, D. J. *Inorg. Chem.* **1994**, *33*, 1382. (b) Gajadhar-Plummer, A. S.; Kahwa, I. A.; White, A. J. P.; Williams, D. J. *Inorg. Chem.* **1999**, *38*, 1745. (c) Matthews, K. D.; Fairman, R. A.; Spence, K. V. N.; Johnson, A.; Kahwa, I. A.; McPherson, G. L.; Robotham, H. *J. Chem. Soc., Dalton Trans.* **1993**, 1719. (d) Howell, R. C.; Spence, K. N. V.; Kahwa, I. A.; Williams, D. J. *J. Chem. Soc., Dalton Trans.* **1998**, 2727.

(40) Komiyama, M.; Takeda, N.; Shigekawa, H. *J. Chem. Soc., Chem. Commun.* **1999**, 1443.

Scheme 1. Summary of Reactions Involving 1-Aziridineethanol and Corresponding Products

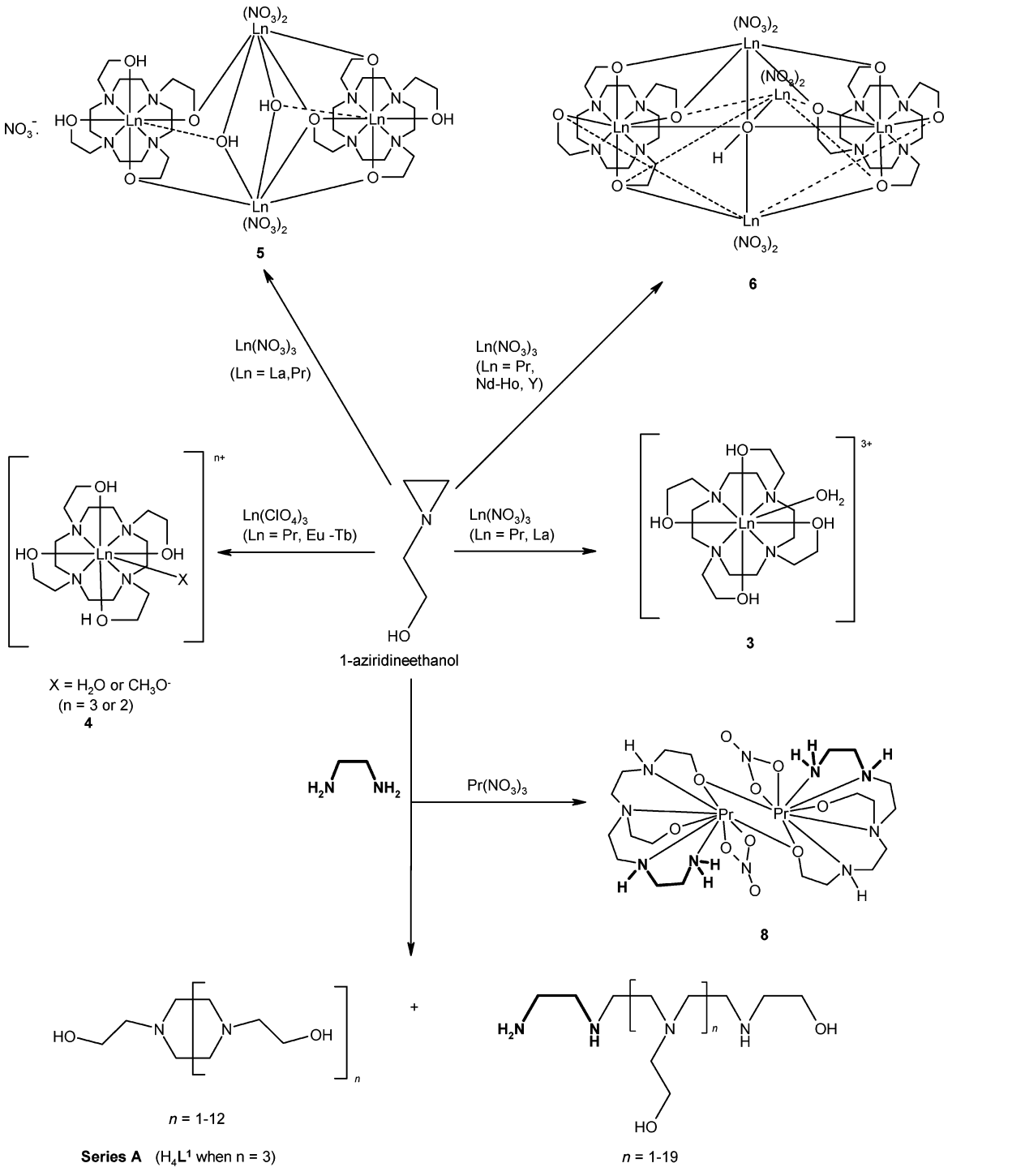

H, 4.7; N, 7.4; Cl, 12.7. Found: C, 23.88; H, 4.82; N, 7.59; Cl, 13.07. FAB MS m/z = 505 corresponding to $[Gd(H_2\mathbf{L^1})]^+$. Anal. Calcd (%) for $\{[EuH_4\mathbf{L^1}(H_2O)](ClO_4)_3\cdot CH_3CN\}\{(H_2O)(HClO_4)\}$ (**4**, Ln = Eu), ($C_{18}H_{44}N_5O_{22}Cl_4Eu$): C, 22.1; H, 4.4; N, 7.2. Found: C, 22.28; H, 4.60; N, 7.13. FAB MS featured a doublet at ca. m/z = 500 corresponding to $[Eu(H_2\mathbf{L^1})]^+$. The terbium complex (**4**, Ln = Tb) was obtained in very low yields. FAB MS indicated a dominant peak (100%) at m/z = 505 corresponding to $[Tb(H_2\mathbf{L^1})]^+$. Single crystal X-ray diffraction studies unequivocally confirmed the presence of the complex and a stoichiometry of $[Tb(H_4\mathbf{L^1})(H_2O)]_4[Tb(H_4\mathbf{L^1})(CH_3O)](ClO_4)_{14}\cdot 12H_2O$ (**4**, Ln = Tb).

$[Pr(H_4\mathbf{L^1})(H_2O)](ClO_4)_3\cdot(CH_3CH_2OH)\cdot 0.3HClO_4$ (4, Ln = Pr). $Pr(ClO_4)_3\cdot nH_2O$ (1.0 mmol) in 50 cm^3 of anhydrous ethanol was added dropwise to a refluxing solution of 1-aziridineethanol (1.65 mmol) in 150 cm^3 of anhydrous ethanol resulting in mild precipitation of a green powder at pH 5. Reflux was continued for 3 days. Filtration yielded a green powder and a light green filtrate. Slow evaporation of the filtrate resulted in green cylindrical crystals of the product in ca. 5% yield. Anal. Calcd (%) for $[Pr(H_4\mathbf{L^1})(H_2O)](ClO_4)_3\cdot EtOH\cdot 0.3HClO_4$ ($C_{18}H_{44.3}N_4O_{19.2}Cl_{3.3}Pr$): C, 23.4; H, 4.7; N, 6.6. Found: C, 23.22; H, 4.65; N, 6.58.

Table 1. Crystallographic Data and Refinement Parameters

data	**3**	**4**	**5**	**6** (LT)	**6** (RT)	**8**
chemical formula	$[C_{16}H_{38}N_4O_5La]$-$[La(NO_3)_6]\cdot 2(CH_3CH_2OH)\cdot 0.5(H_2O)$	$[(C_{16}H_{36}N_4O_4)$-$Tb(OH_2)]_4[(C_{16}$-$H_{36}N_4O_4)Tb(OCH_3)]$-$[ClO4]_{14}\cdot 12H_2O$	$C_{32}H_{67}La_4N_{13}$-$O_{25}\cdot H_2O$	$C_{32}H_{65}N_{14}O_{27}Nd_5\cdot$ (CH_3CH_2OH)	$C_{32}H_{65}N_{14}O_{27}$-$Nd_5\cdot(CH_3CH_2OH)$	$C_{10}H_{24}N_5O_5Pr$
solvent	CH_3CH_2OH	CH_3OH	CH_3CH_2OH	CH_3CH_2OH	CH_3CH_2OH	CH_3CH_2OH
fw	1117.53	4248.63	1607.64	1845.25	1845.25	435.25
space group	*Pna*2$_1$ (No. 33)	*P*4/*n* (No. 85)	*P*2$_1$/*c* (No. 14)	*C*2/*c* (No. 15)	*C*2/*c* (No. 15)	*C*2/*c* (No. 15)
T (°C)	−100	−100	−173	−163	20	−173
a (Å)	23.647(3)	23.1578(10)	19.9955(5)	21.005(1)	21.291(3)	19.6160(6)
b (Å)	11.4698(14)	23.1578(10)	14.3228(3)	11.741(1)	11.815(2)	14.6034(4)
c (Å)	15.802(3)	14.9189(10)	20.2977(5)	23.856(1)	23.997(4)	14.8984(3)
α (deg)	90	90	90	90	90	90
β (deg)	90	90	93.669(3)	91.25(1)	91.64(1)	119.596(14)
γ (deg)	90	90	90	90	90	90
V (Å^3)	4285.8(11)	8000.8(7)	5801.2(2)	5881.8(4)	6034(2)	3710.98(17)
Z	4	2	4	4	4	8
D_{calcd} (g cm^{-3})	1.732	1.764	1.841	2.084	2.031	1.558
λ (Å)	1.54178	1.54178	0.71073	0.71073	0.71073	0.71073
μ (mm^{-1})	16.045	13.749	2.973	4.43	4.32	2.650
indep data	3425	5867	13235	6648	5322	4240
obsd data	2815	3861	8896	4537	3503	3284
params	497	628	676	419	418	206
R1[a]	0.1037	0.0791	0.0417	0.059	0.059	0.0339
wR2[b]	0.2728	0.2035	0.0889	0.128	0.126	0.0842

[a] $R1 = \sum||F_o| - |F_c||/\sum|F_o|$. [b] $wR2 = \{\sum[w(F_o^2 - F_c^2)^2]/\sum[w(F_o^2)^2]\}^{1/2}$; $w^{-1} = \sigma^2(F_o^2) + (aP)^2 + bP$.

[(Ln(H$_2$L^1))$\{$Ln(NO$_3$)$_2$(μ_3-OH)$\}_2$(Ln(HL^1))](NO$_3$)·EtOH·2H$_2$O (5). Ln(NO$_3$)$_3\cdot n$H$_2$O (1.0 mmol) in 45 cm^3 of ethanol was added dropwise over 24 h to a solution of 1-aziridineethanol (2.5 mmol) in 100 cm^3 of ethanol. After 2^1/$_2$ days of reflux, ethylenediamine (2.0 mmol) in 50 cm^3 ethanol was added (as a base) and reflux continued. Crystallization of [(Ln(H$_2$L^1))$\{$Ln(NO$_3$)$_2$(μ_3-OH)$\}_2$(Ln(HL^1))](NO$_3$)·CH$_3$CH$_2$OH·2H$_2$O (Ln = La (**5**, Ln = La), Pr (**5**, Ln = Pr)) ensued within 2 days in ca. 32% yield. Anal. Calcd (%) for Ln = La ($C_{34}H_{79}N_{13}O_{28}La_4$): C, 24.4; H, 4.8; N, 10.9. Found: C, 24.27; H, 4.57; N, 10.53. Anal. Calcd (%) for Ln = Pr, ($C_{34}H_{79}N_{13}O_{29}Pr_4$): C, 24.3; H, 4.6; N, 10.8. Found: C, 24.49; H, 4.39; N, 10.56. Addition of ethylenediamine is not required when Ln = Pr.

[$\{$Ln(NO$_3$)$_2\}_3$(Ln(L^1))$_2$(μ_5-OH)]·*x*H$_2$O·*y*CH$_3$CH$_2$OH (Ln = Pr, Nd, Sm−Ho, Y) (6). Ln(NO$_3$)$_3\cdot n$H$_2$O (1.0 mmol) in 50 cm^3 of anhydrous ethanol was added dropwise over 24 h to a refluxing solution of 1-aziridineethanol (2.5 mmol) in 150 cm^3 of anhydrous ethanol resulting in a cloudy solution. Reflux was maintained, and formation of cube- or needlelike crystals of [$\{$Ln(NO$_3$)$_2\}_3$(Ln(**L^1**))$_2$-(μ_5-OH)]·*x*H$_2$O·*y*CH$_3$CH$_2$OH (Ln = Pr, Nd, Sm−Ho) occurred within 2 days in yields of 15−99%. Crystals of the pentanuclear Y^{III} complex were isolated only after slow evaporation of the solvent at the end of the reflux reaction. The yields and solvent composition (*x* and *y*) were dependent on the nature of Ln^{III} ions used. The composition, yields, and elemental analyses are shown in the Supporting Information, Table S1. For rare earth ions smaller than Ho^{III}, no crystals of the pentanuclear complex were deposited during reflux or after slow evaporation of the solvent (except for the Y^{III} complex).

Pr^{III} Complexes of H$_2$L^2. Pr(NO$_3$)$_3\cdot n$H$_2$O (1.0 mmol) in 50 cm^3 of ethanol was added dropwise over 2 h to a refluxing solution of 1-aziridineethanol (2.0 mmol) in 100 cm^3 of ethanol resulting in precipitation of a light green powder. Reflux and vigorous stirring were continued for 1 h, then ethylenediamine (1.0 mmol) in 50 cm^3 ethanol was added, and then reflux and agitation continued for 3 days. Filtration yielded a green powder (**7**) of undefined stoichiometry. IR (KBr disk; cm^{-1}): 1384, ionic NO$_3^-$. FAB MS of **7**: *m*/*z* = 435 ([Pr(HL^2)(NO$_3$)]$^+$), 373 ([Pr(**L^2**)]$^+$) and 235 ([H$_3$L^2]$^+$). Slow evaporation of the light green filtrate resulted in green crystals of [Pr(**L^2**)(NO$_3$)]$_2\cdot$HNO$_3\cdot$3H$_2$O (**8**) in ca. 4% yield. Anal. Calcd (%) for [Pr(**L^2**)(NO$_3$)]$_2\cdot$HNO$_3\cdot$3H$_2$O, ($C_{20}H_{55}N_{11}O_{16}$-Pr$_2$): C, 24.3; H, 5.6; N, 15.6. Found: C, 23.99; H, 5.15; N, 15.44%. IR (cm^{-1}): bidentate NO$_3^-$, 1309, 1438; ionic NO$_3^-$, 1384; N−H, 3237−3342. Complete evaporation of the solvent from the filtrate yielded a green paste (**9**). FAB MS of **9**: *m*/*z* = 373 ([Pr(**L^2**)]$^+$), 436 ([Pr(HL^2)(NO$_3$)]$^+$), 499 ([Pr(H$_2$L^2)(NO$_3$)$_2$]$^+$.

X-ray Crystal Structure Determinations. Data for compounds **5**, **6**(LT) (low temperature structure), and **8** were collected on a Nonius Kappa-CCD diffractometer using monochromated Mo Kα radiation. Each data set was measured using a combination of *φ* scans and *ω* scans with *κ* offsets. The data were integrated and scaled using the Denzo-SMN package.[41a] The structures were solved and refined using SHELXTL V5.1[41b] in full-matrix least-squares refinement based on F^2. Data for compounds **3** and **4** were determined using a Siemens P4/RA diffractometer while the room temperature data set for **6**(RT) was collected using a Siemens P4/PC. Crystallographic data and refinement parameters are given in Table 1. All other data are available as Supporting Information. The polarity of the structure of **3** was determined by a combination of *R*-factor tests [R1$^+$ = 0.1037, R1$^-$ = 0.1080] and by use of the Flack parameter [x^+ = +0.16(5), x^- = +0.84(5)]. Data have been deposited with the CCDC.

Results and Discussion

Cyclic and Acyclic Oligomeric Chelates (Series A and B). The reaction between 1-aziridineethanol and a simple diamine, ethylenediamine (en), was initially explored as a route to novel and diverse poly(amino-alkoxide) ligands. The fast atom bombardment mass spectrum (FAB MS) (Figure 1) of the product (**2**) resulting from the reaction between 1-aziridineethanol and en reveals dramatically the considerable potential of the ring-opening amination of 1-aziri-

(41) (a) Otwinowski, Z.; Minor, W. *Macromolecular Crystallography, Part A*; Carter, C. W., Sweet, R. M., Eds.; Methods in Enzymology 276; Academic Press: London, 1997; pp 307−326. (b) Sheldrick, G. M. *SHELXTL/PC*, Version 5.1, Windows NT Version; Bruker AXS Inc.: Madison, WI, 2001.

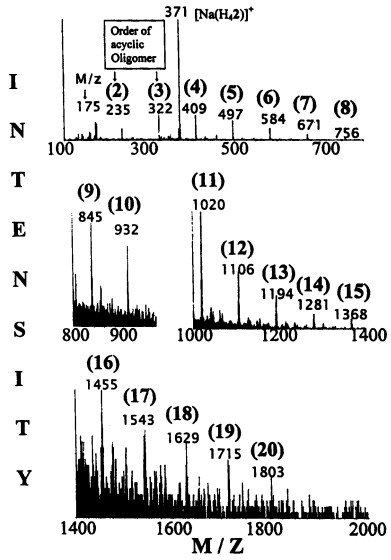

Figure 1. FAB MS of **2** from ring-opening oligomerization of 1-aziridineethanol in the presence of ethylenediamine. Oligomerization orders for acyclics of series B (the value of $(n+1)$ in the formula in Scheme 1) are bold and in parentheses.

dineethanol as a rich source of interesting cyclic and acyclic poly(amino-alkoxide) chelates.

There are two series of oligomeric chelates: an acyclic one (series B), which is extensive, and the cyclic series A (Scheme 1) of which the sodium complex of the tetramer ($H_4\mathbf{L^1}$) is the most prominent ($m/z = 371$). Ring-opening cyclooligomerization of 1-aziridineethanol is the origin of cyclic oligomers of series A. As expected,[8,12−14] when 1-aziridineethanol is refluxed alone in ethanol, only peaks due to cyclic oligomers (series A) and their sodium(I) compounds with $n \leq 12$ (Scheme 1) are found in the FAB MS of the resulting product (**1**) (Figure 1S, Supporting Information). The series obtained here is more extensive (maximum $n = 12$) than that of Ham et al. ($n = 9$).[13] Again, the Na(I) complex of $H_4\mathbf{L^1}$ is the dominant species in the mass spectrum. We propose a process summarized in Scheme 2 for the ring-opening of 1-aziridineethanol and subsequent oligomerization to various members of series A and series B. We hypothesize that the principal reaction is the successive ring-opening oligomerization of 1-aziridineethanol to produce acyclic intermediate oligomers, which at some point is terminated by cyclization (to form series A) or N-alkylation of ethylenediamine (to yield acyclic series B).

The facile nature of the syntheses and the potential to isolate novel macromolecular poly(amino-alkoxides) makes this procedure attractive for building diverse chelates for metal ions. The subtle differences in ionic radii, ionic potential, Lewis acidity, and coordination requirements of metal ions across the Ln^{III} series have significant consequences in molecular recognition events.[37,39a−c] These subtle differences might be exploited to dictate the ligand assembly, the specific chelate that can be bound to the Ln^{III} ions, and the order of nuclearity of resulting complexes[33a,42] as well as other structural details. Lanthanide complexes of DOTA are generally thermodynamically stable and kinetically inert[1c] and so is the $[Eu(H_4\mathbf{L^1})]^{3+}$ complex (dissociation in water at physiological temperature (37 °C) and pH 6.8: $t_{1/2} = 18$ days, $k \approx 4.4 \times 10^{-7}$ s^{-1}).[15] Therefore, the cyclo-oligomerization of 1-aziridineethanol in the presence of Ln^{III} ions was investigated with the anticipation that Ln^{III} ions would form isolable thermodynamically stable and kinetically inert complexes[15−21,43] of the major product $H_4\mathbf{L^1}$. The ethylenediamine-terminated oligomerization of 1-aziridineethanol was also investigated as a route to novel acyclic Ln^{III} complexes of Series B.

Lanthanide(III) Complexes of $H_4\mathbf{L^1}$. Indeed, cyclo-oligomerization of 1-aziridineethanol in the presence of Ln^{III} ions produces a class of complexes of $H_4\mathbf{L^1}$ ranging from mononuclear to pentanuclear clusters, depending on the nature of Ln^{III} salts used and the degree of protonation of the chelate (Scheme 1). The solution chemistry of the mononuclear Ln^{III} complexes of $H_4\mathbf{L^1}$ has been previously investigated;[15,43] however, there has been a distinct absence of structurally characterized lanthanide complexes of $H_4\mathbf{L^1}$. This is an important gap given the very exciting efficiency of $[Ln(H_4\mathbf{L^1})]^{3+}$ in the cleavage of nucleic acids such as RNA, which is well documented.[15−21] Crystalline mononuclear, tetranuclear, and pentanuclear complexes were obtained in forms suitable for single crystal X-ray analyses, and this is the first report of structurally characterized complexes of $H_4\mathbf{L^1}$, save for those of alkali metal ions.[25]

Mononuclear Ln^{III} Complexes of $H_4\mathbf{L^1}$. The assembly of $[Ln(H_4\mathbf{L^1})(H_2O)][Ln(NO_3)_6]$ from simple $Ln(NO_3)_3{\cdot}nH_2O$ and 1-aziridineethanol components occurs at pH 5−6 with the larger lanthanides (Ln = La and Pr). The role of Ln^{III} ions in the formation of chelate $H_4\mathbf{L^1}$ (i.e., template or just a versatile binder) is not clear because this chelate is the major product of nontemplate reactions as well.[13] Structural analyses of the lanthanum complex by single crystal X-ray diffraction conclusively established the identity of the complex as $\{[La(H_4\mathbf{L^1})(H_2O)][La(NO_3)_6]{\cdot}2CH_3CH_2OH{\cdot}0.5H_2O\}$ (**3**) (Figure 2).

The crystal structure reveals the presence of $[La(H_4\mathbf{L^1})(H_2O)]^{3+}$ cations with La^{III} ions in a distorted monocapped square antiprimatic 9-fold coordination environment (Figure 2(top right)) and a distorted icosahedron of the $[La(NO_3)_6]^{3-}$ anion (Figure 2(top left)). The absolute stereochemistry of the $H_4\mathbf{L^1}$ chelate in the complex is Δ for the helicity of the pendant CH_2CH_2OH arms and $\delta\delta\delta\delta$ for the ring chirality (hereafter $\Delta(\delta\delta\delta\delta)$) (Supporting Information Figure 2S). Ln^{III} complexes of the heavy Ln^{III} ions were not isolated presumably because of the relatively greater difficulty in forming the corresponding 12-coordinate icosahedral $[Ln(NO_3)_6]^{3-}$ complex. Of the approximately 27 entries for $[Ln(NO_3)_6]^{3-}$ in the Cambridge Structure Database,[44] there are only four reports for which Ln is not La, Ce, Pr, or Nd; those four are for Ln = Eu[45] (three) and Gd[46] (one). Selected interatomic distances for compound **3** are given in Table 2.

(42) Franklin, S. J.; Raymond, K. N. *Inorg. Chem.* **1994**, *33*, 5794.

(43) Pittet, P.-A.; Fruh, D.; Tissieres, V.; Bünzli, J.-C. G. *J. Chem. Soc., Dalton Trans.* **1997**, 895.

(44) *Cambridge Structure Data Centre Database*, April 2003 release.

(45) Yuguo, F.; Jingsheng, Y.; Pinzhe, L.; Shongsheng, J.; Fenglan, Y.; Shugong, Z.; Jiazhan, N. *Yingyong Huaxue (Chin. J. Appl. Chem.)* **1986**, *3*, 35.

Scheme 2. Postulated Pathways to Series A and Series B

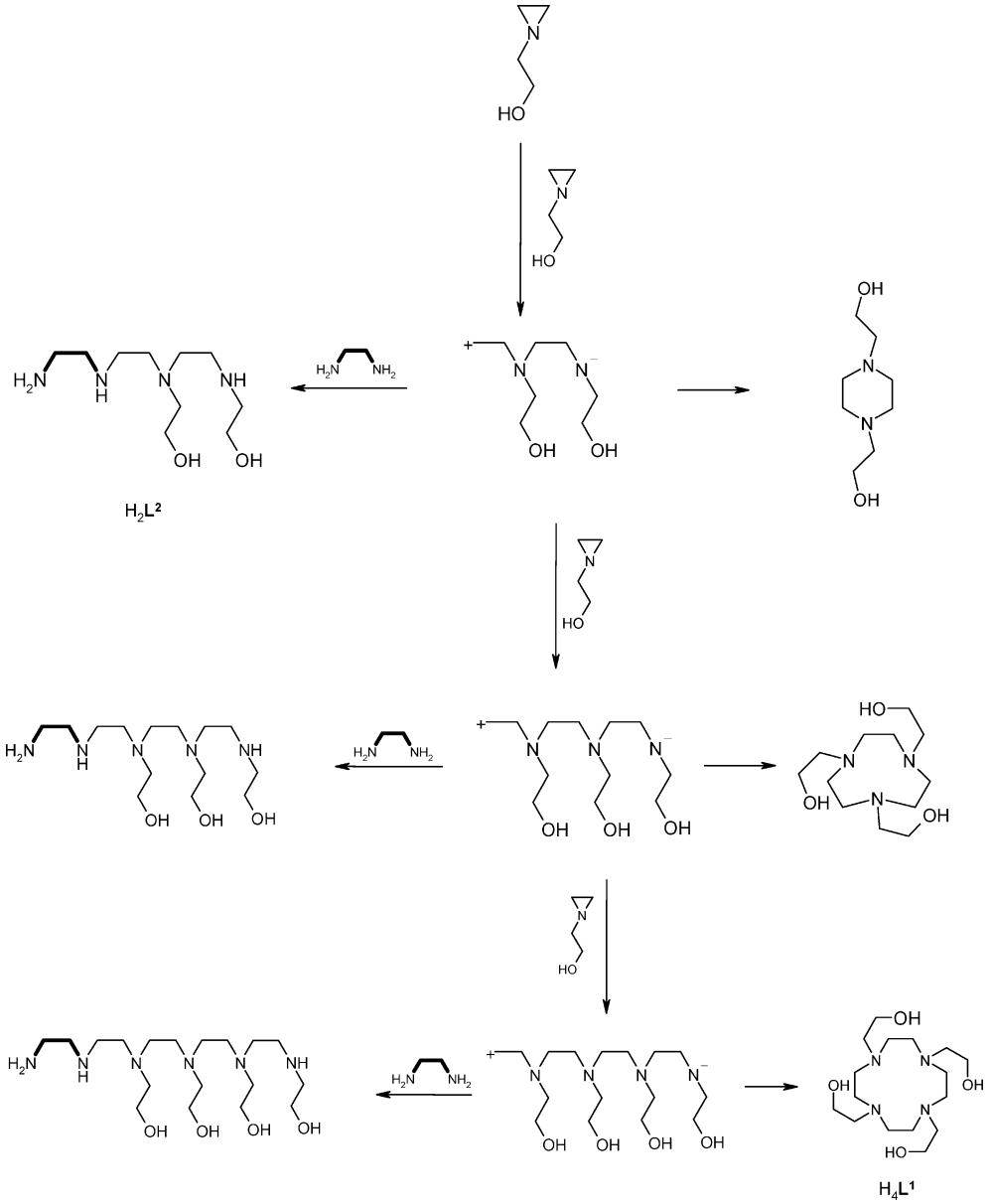

Nitrate anions have the propensity to coordinate to Ln^{III} cations and may thus influence the kind of complexes formed between Ln^{3+} cations and chelate $H_4\mathbf{L^1}$. The potential of perchlorate anions, which are relatively large and spherical and have little tendency to coordinate to Ln^{III} ions, was thus explored. Complexes of lanthanide(III) perchlorates are formed at pH 5−6, and the Pr, Eu, and Gd complexes adopt the general stoichiometry $[Ln(H_4\mathbf{L^1})(H_2O)](ClO_4)_3 \cdot X$, where X is solvent.

Because of the complexity of the stoichiometries of these compounds, we studied their luminescence behavior to determine if the products have lanthanide(III) ions in single or multiple and significantly different crystal field environments. For the Eu^{III} compounds, differences in crystal field environments are readily indicated by a multiplicity of peaks corresponding to the $^5D_0 \rightarrow {}^7F_0$ singlet transition in the emission spectra.[37] The occurrence of such multiple environments in a single well defined lattice might also be inferred from the $^5D_0 \rightarrow {}^7F_j$ emission decay behavior.[7b] The emission spectrum of crystals of $\{[Eu(H_4\mathbf{L^1})(H_2O)](ClO_4)_3 \cdot (CH_3CN)\} \cdot \{(H_2O)(HClO_4)\}$ features one prominent $^5D_0 \rightarrow {}^7F_0$ transition at 579.5 nm and a minor one at 583 nm (see arrow Figure 3) while that of its aqueous solution (Figure 3) features the major $^5D_0 \rightarrow {}^7F_0$ peak only. Its prominent relative intensity and the spectral profile, in general, are reflective of the low site symmetry of the Eu^{III} ion, i.e., ca. C_{4v}, as determined crystallographically for the Tb^{3+} complex. The corresponding excitation spectra (not shown) feature the major $^5D_0 \rightarrow {}^7F_0$ peak only. The solution stability of the complex is reflected in the absence of major changes in the spectra recorded when the complex is dissolved in D_2O. There are no significant changes in the coordination environment of the metal ion upon dissolution, which is consistent with the known solution kinetic stability of the $[LnH_4\mathbf{L^1}]^{3+}$ complex.[7b]

(46) Nicolo, F.; Bünzli, J.-C. G.; Chapuis, G. *Acta Crystallogr., Sect. C: Cryst. Struct. Commun.* **1988**, *44*, 1733.

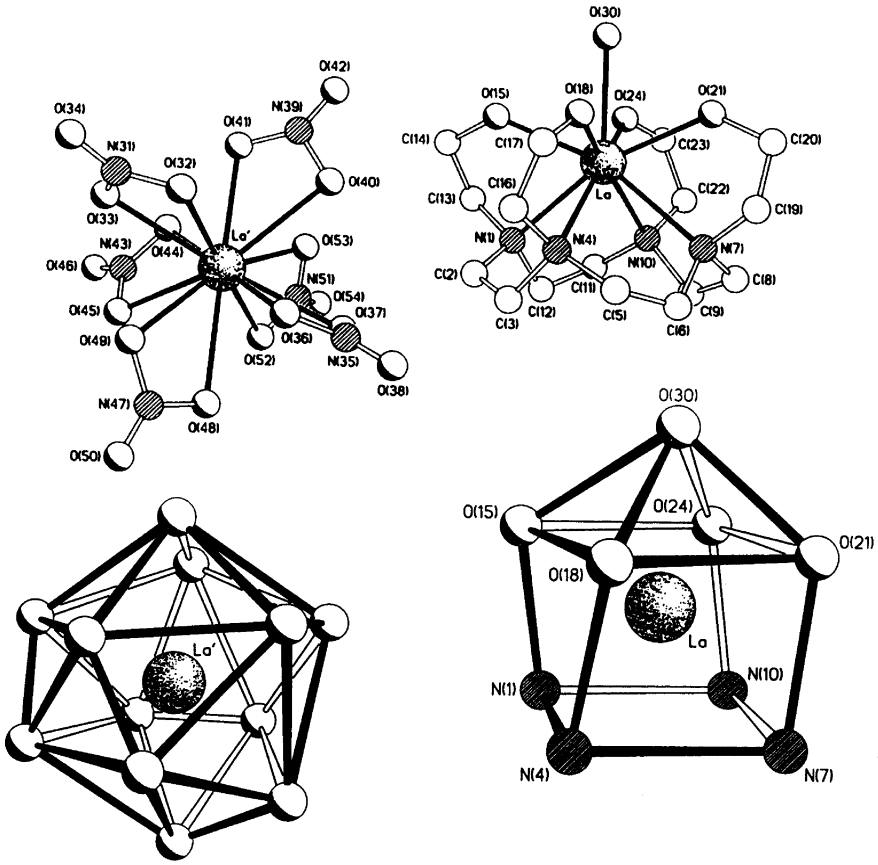

Figure 2. Structures of $[La(H_4\mathbf{L}^1)(H_2O)]^{3+}$ and $[La(NO_3)_6]^{3-}$ ions in compound **3** and the coordination polyhedra around the La^{III} ions (below).

Table 2. Selected Interatomic Distances (Å)

3		**4**		**5**				**6** (110 K)		**8**	
La−N(1)	2.69(2)	Tb−N(1)	2.619(14)	La(1)−O(2)	2.441(3)	La(3)−N(8)	2.875(4)	Nd(1)−N(1)	2.684(8)	Pr(1)−N(1)	2.637(4)
La−N(4)	2.65(2)	Tb−N(4)	2.60(2)	La(1)−O(3)	2.576(3)	La(3)−O(5)	2.460(3)	Nd(1)−N(4)	2.725(8)	Pr(1)−N(2)	2.645(4)
La−N(7)	2.71(2)	Tb−N(7)	2.612(14)	La(1)−O(5)	2.428(3)	La(3)−O(6)	2.409(3)	Nd(1)−N(7)	2.731(9)	Pr(1)−N(3)	2.700(3)
La−N(10)	2.69(3)	Tb−N(10)	2.611(13)	La(1)−O(9)	2.500(3)	La(3)−O(7)	2.561(3)	Nd(1)−N(10)	2.762(10)	Pr(1)−N(4)	2.661(3)
La−O(15)	2.40(4)	Tb−O(15)	2.446(12)	La(1)−O(10)	2.534(3)	La(3)−O(8)	2.571(3)	Nd(1)−O	2.7538(5)	Pr(1)−O(1)	2.548(3)
La−O(18)	2.36(4)	Tb−O(18)	2.392(13)	La(1)−O(11)	2.689(4)	La(3)−O(10)	2.448(3)	Nd(1)−O(15)	2.435(6)	Pr(1)−O(2)	2.368(3)
La−O(21)	2.40(3)	Tb−O(21)	2.39(2)	La(1)−O(12)	2.699(4)	La(3)−O(14)	2.661(4)	Nd(1)−O(18)	2.436 (7)	Pr(1)−O(2)#1	2.397(3)
La−O(24)	2.35(4)	Tb−O(24)	2.446(14)	La(1)−O(14)	2.661(4)	La(4)−N(1)	2.856(5)	Nd(1)−O(21)	2.410(6)	Pr(1)−O(3)	2.645(3)
La−O(30)	2.57(3)	Tb−O(30)	2.549(10)	La(1)−O(15)	2.644(4)	La(4)−N(2)	2.787(5)	Nd(1)−O(24)	2.425(6)	Pr(1)−O(4)	2.605(3)
La′−O(33)	2.61(2)	Tb′−N(31)	2.669(9)	La(2)−O(3)	2.594(3)	La(4)−N(3)	2.801(5)	Nd(2)−O	2.6146(5)	Pr(1)···Pr(1)#1	3.9485(4)
La′−O(49)	2.58(2)	Tb′−O(36)	2.401(7)	La(2)−O(4)	2.456(4)	La(4)−N(4)	2.795(5)	Nd(2)−O(15)#1	2.433(6)		
La′−O(32)	2.59(2)	Tb′−O(37)	2.43(2)	La(2)−O(6)	2.412(3)	La(4)−O(1)	2.501(3)	Nd(2)−O(18)	2.403(6)		
La′−O(36)	2.62(2)			La(2)−O(9)	2.509(3)	La(4)−O(2)	2.421(3)	Nd(2)−O(21)	2.460(6)		
La′−O(45)	2.64(2)			La(2)−O(10)	2.508(3)	La(4)−O(3)	2.523(3)	Nd(2)−O(24)#1	2.440(7)		
La′−O(44)	2.64(2)			La(2)−O(17)	2.612(4)	La(4)−O(4)	2.509(3)	Nd(2)−O(26)	2.591(7)		
La′−O(53)	2.72(2)			La(2)−O(18)	2.682(4)	La(4)−O(9)	2.542(3)	Nd(2)−O(27)	2.578(6)		
La′−O(33)	2.61(2)			La(2)−O(21)	2.680(4)	La(1)···La(2)	3.7861(4)	Nd(2)−O(30)	2.550(7)		
La′−O(37)	2.62(2)			La(2)−O(22)	2.632(4)	La(1)···La(3)	4.123(4)	Nd(2)−O(31)	2.582(7)		
La′−O(52)	2.64(2)			La(3)−N(5)	2.785(4)	La(1)···La(4)	3.8052(4)	Nd(3)−O	2.5937(9)		
La′−O(48)	2.66(2)			La(3)−N(6)	2.784(4)	La(2)···La(3)	4.0623(4)	Nd(3)−O(15)#1	2.533(7)		
La′−O(40)	2.73(3)			La(3)−N(7)	2.814(4)	La(3)···La(4)	6.6293(4)	Nd(3)−O(18)#1	2.616(7)		
								Nd(3)−O(21)	2.569(7)		
								Nd(3)−O(24)	2.608(8)		
								Nd(3)−O(34)	2.54(2)		
								Nd(3)−O(35)	2.56(2)		
								Nd(3)−O(38)	2.556(13)		
								Nd(3)−O(39)	2.487(13)		
								Nd(1)···Nd(2)	3.7883(7)		
								Nd(1)···Nd(3)	3.7832(10)		
								Nd(1)···Nd(3)#1	3.7826(10)		
								Nd(2)···Nd(3)	3.6597(10)		

Upon direct excitation into the major absorption at about 579 nm (emission monitored at 612.5 nm), single exponential decay behavior of marginal temperature dependency prevails (decay rate = 5.2×10^3 and 4.3×10^3 s^{-1} at 293 and 77 K, respectively). The decay behavior of the complex in both H_2O and D_2O solutions is single exponential (decay rates =

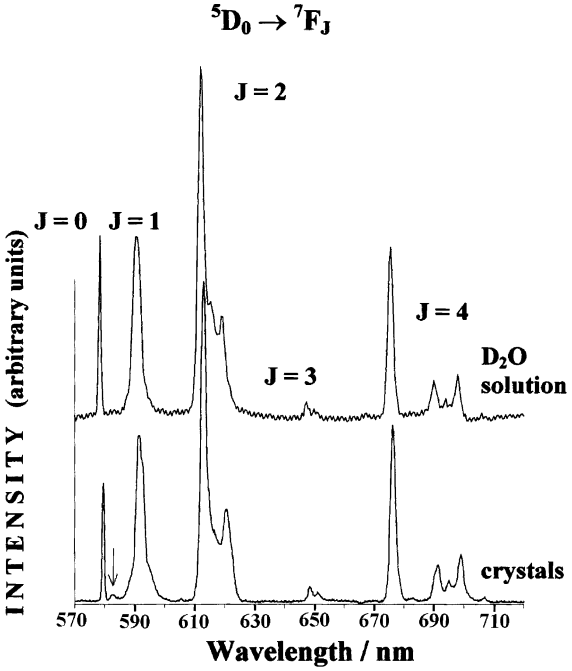

Figure 3. Luminescence spectra at 77 K of $[EuH_4\mathbf{L^1}(H_2O)]^{3+}$ in crystalline (bottom) and frozen D_2O solution (top); $\lambda_{exc} = 393$ nm. Arrow points to the minor $^5D_0 \rightarrow {}^7F_0$ peak (see text).

5.2×10^3 and 1.0×10^3 s^{-1}, respectively). The decay rates of crystalline and aqueous $\{[Eu(H_4\mathbf{L^1})(H_2O)](ClO_4)_3 \cdot CH_3CN\}\{(H_2O)(HClO_4)\}$ compare well with those of Chappel et al. ($4.75-5.32 \times 10^3$ s^{-1} for solutions of $[Eu(H_4\mathbf{L^1})(H_2O)](CF_3SO_3)_3$ at pH 6.3−8.6).[19] Application of the well-known Sudnick−Horrocks equation[21] for calculating the number of coordinated O−H oscillators yields 6.8 O−H oscillators instead of the expected 6 in $[Eu(H_4\mathbf{L^1})(H_2O)]^{3+}$, but this is within the accuracy expected from use of the Sudnick−Harrocks equation, which is accurate to within ±0.5 H_2O or one O−H oscillator.

The emission decay behavior of Tb^{III} ($^5D_4 \rightarrow {}^7F_j$) in the terbium(III) complex was also single exponential and marginally temperature dependent (decay rates, 9.3×10^2 and 9.2×10^2 s^{-1} at 293 and 77 K, respectively). If indeed there are two different crystallographic Ln^{3+} sites, then the single exponential luminescence decay behavior is consistent with energy migration among similar sites being fast while energy transfer among different sites is inefficient, as found when energy transport is in the dynamic regime. It was thus necessary to determine the structure of the series in order to establish unequivocally the nature of its members. The terbium(III) product was suitable for single crystal X-ray analyses and confirmed the presence of two different sites of Tb^{III} in $[Tb(H_4\mathbf{L^1})(H_2O)]_4[Tb(H_4\mathbf{L^1})(OCH_3)](ClO4)_{14} \cdot 12H_2O$ (**4**).

The crystal structure shows a mononuclear complex $[Tb(H_4\mathbf{L^1})(H_2O)]_4[Tb(H_4\mathbf{L^1})(OCH_3)][ClO4]_{14} \cdot 12H_2O$ (**4**) in which the Tb^{III} ions are nine-coordinate and are in two different environments (Figure 4) as suggested by the luminescence behavior of the europium(III) compound (Figure 3). The coordination polyhedra at both $[Tb(H_4\mathbf{L^1})(H_2O)]^{3+}$ and $[Tb(H_4\mathbf{L^1})(OCH_3)]^{2+}$ sites are distorted monocapped square antiprisms of ca. C_{4v} symmetry. Each $[Tb(H_4\mathbf{L^1})(H_2O)]^{3+}$ site

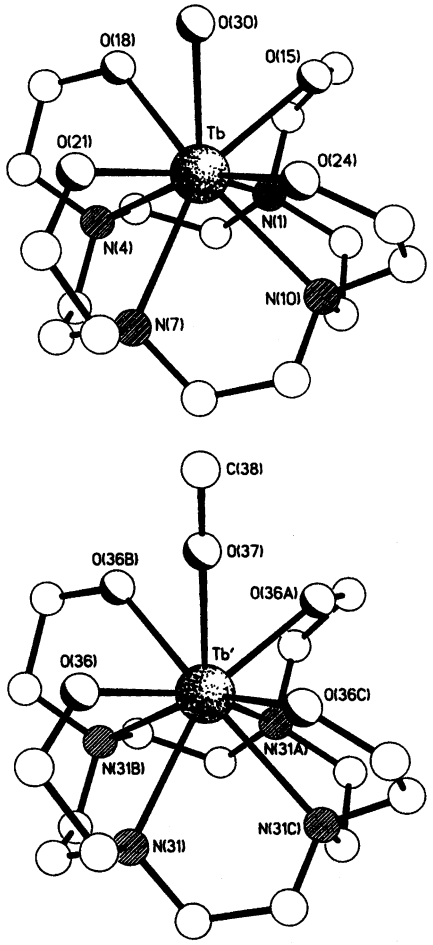

Figure 4. Structures of cations $[Tb(H_4\mathbf{L^1})(OH_2)]^{3+}$ (top (Tb)) and $[Tb(H_4\mathbf{L^1})(OCH_3)]^{2+}$ (bottom (Tb′)) in compound **4** (m_1 $[TbH_4\mathbf{L^1}(H_2O)]^{3+}$ enantiomer, perchlorate anions, and water molecules are omitted for clarity).

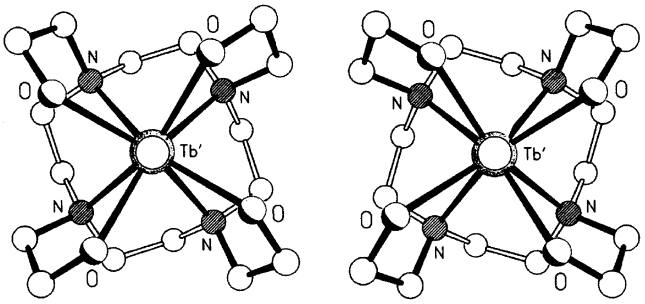

Figure 5. View down the C_4 axis of the m_1 isomer of $[TbH_4\mathbf{L^1}(H_2O)]^{3+}$ showing the (Δ) lay-out of the pendant arms and the ($\delta\delta\delta\delta$) conformation of the ring (left), and the m_2 isomer of $[TbH_4\mathbf{L^1}(H_2O)]^{3+}$ showing the (Λ) lay-out of the pendant arms and the ($\lambda\lambda\lambda\lambda$) conformation of the ring (right). Note: Orientation of N relative to O atoms is closer to prismatic for isomers m_1 and m_2 and antiprismatic for M_1 and M_2 (see Vaira, M. D.; Stoppion, P. *New J. Chem.* **2002**, *26*, 136).

features a disorder ratio 55:45 between the two possible enantiomers, but crystallographic inversion symmetry which relates the enantiomers precludes identification of the more favorable isomers, Δ($\delta\delta\delta\delta$) or Λ($\lambda\lambda\lambda\lambda$), as shown in Figure 5. The absolute stereochemistry at the $[Tb(H_4\mathbf{L^1})(OCH_3)]^{2+}$ cation is Λ($\lambda\lambda\lambda\lambda$). The N_4O_4 stagger angle is ca. 22° while the torsional twist in the pendant CH_2CH_2OH arms is ca. 43°. The CH_3-O-Tb angle (C(38)−O(37)−Tb′) is linear, 180°, and larger than literature terminal $Ln^{III}-O-CH_3$ angles involving coordinated CH_3OH molecules, which usually fall

in the range ca. 120−145° with only two cases of larger angles (ca. 159° and 169°)[47,48] reported so far.

The structures of **3** and **4** exhibit some disorder in their cores which, in the case of the Tb complex, was resolved into two alternative orientations (both with the same geometry) while for the La complex equivalent bond lengths had to be constrained. The structures as illustrated, however, are a true representation of the coordination geometry.

It is clear that when cyclooligomerization of 1-aziridineethanol occurs in the presence of Ln^{III} ions under very weakly acidic conditions (pH of ca. 5−6) the principal products are complexes of $[Ln(H_4\mathbf{L^1})(X)]^{y+}$ cations (y dependent on the nature and charge on X, Scheme 1). It was therefore interesting to determine the type of products formed when cyclo-oligomerization of 1-aziridineethanol occurs under more basic conditions in light of the pK_a (7−7.5) of the pendant alcohol groups.[15]

Polynuclear Lanthanide(III) Complexes of $[H_{4-x}\mathbf{L^1}]^{x-}$. The cyclooligomerization of 1-aziridineethanol at pH 6−7 (achieved with en) in the presence of La^{III} nitrate results in a self-assembled tetranuclear asymmetric cluster $[(La(H_2\mathbf{L^1}))\{La(NO_3)_2(\mu_3\text{-}OH)\}_2(La(H\mathbf{L^1}))](NO_3)\cdot CH_3CH_2OH\cdot 2H_2O$ (**5**). The anionic sites of ligands $[H_2\mathbf{L^1}]^{2-}$ and $[H\mathbf{L^1}]^{3-}$ are coordinatively unsaturated and therefore readily bridge the metal ions. The synthesis of tetranuclear clusters of the smaller Pr^{III} ions does not require the presence of the base en. A careful inspection of the reaction with Pr^{III} indicates the tetranuclear cluster is a kinetic product formed at least 3 days after the formation of the mononuclear species (which can typically be isolated by rapid evaporation of the solvent within hours of starting the reaction). Complete deprotonation of the macrocyclic chelate occurs with prolonged reflux (at least 1 week) to yield self-assembled pentanuclear complexes of $[\mathbf{L^1}]^{4-}$, $[\{Pr(NO_3)_2\}_3(Pr(\mathbf{L^1}))_2(\mu_5\text{-}OH)]$. Scheme 3 indicates the intermediates isolated in the process of forming the pentanulear Pr^{III} cluster. These intermediates were characterized by elemental analyses and FAB MS and featured crystal morphologies which were consistent with those of the structurally characterized complexes.

For the smaller lanthanides (Ln = Nd, Sm−Ho), full deprotonation of the chelate and formation of pentanuclear complexes, $[\{Ln(NO_3)_2\}_3(Ln(\mathbf{L^1}))_2(\mu_5\text{-}OH)]$ (**6**), proceeds readily. Yields of the pentanuclear clusters are generally high (15−91% without base; 59−99% when en is used as a base).

The assembly of the clusters is the result of a complex interplay of several factors.[37] It is evident from the structure of **5** that deprotonation of the alkoxide pendant arms of chelate $H_4\mathbf{L^1}$ promotes the ability of alkoxide sites to form bridges to Ln^{III} ions while protonated alkoxy pendant arms are coordinatively saturated and do not bridge the Ln^{III} ions. The reaction conditions for the syntheses of the tetranuclear and pentanuclear clusters are very similar; what determines the nature of the product formed is the relative Lewis acidity of Ln^{III} ions, the smaller and harder Lewis acids being more

Scheme 3. Observed Synthetic Pathway to the Pr^{III} Pentanuclear Cluster[a]

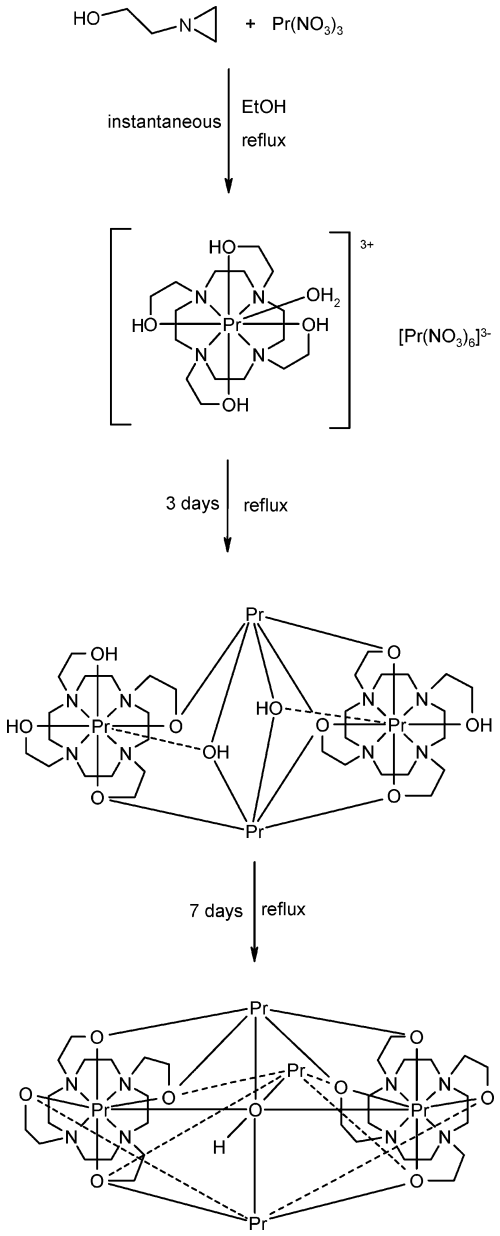

[a] Nitrate anions removed for clarity.

able to displace the hydroxyl protons from $H_4\mathbf{L^1}$. The stoichiometry of the reactants and the pH of the reaction medium are of limited influence, though yields tend to be greater at higher pH. For example, when an 8:4 1-aziridineethanol/Ln^{III} ratio was attempted (in the absence of en), the product remained pentanuclear throughout the series (Ln = Nd, Sm−Ho, Y). When an 8:5 1-aziridineethanol/Ln^{III} ratio was attempted with La^{III}, in the presence of en to foster complete deprotonation, the tetranuclear complex persisted after several weeks of reflux. Lanthanide(III) ions that are smaller than Ho^{III} and Y^{III} formed intractable products. The role of the $(\mu_5\text{-}OH)^-$ group as a molecular glue is of primary importance to these unique molecules ($[\{Ln(NO_3)_2\}_3(Ln(\mathbf{L^1}))_2(\mu_5\text{-}OH)]$). The Ln^{III} perchlorates have a different chemistry (partly due to the large size and weak coordination

(47) Lachkar, M.; Tabard, A.; Brandes, S.; Guilard, R.; Atmani, A.; De Cian, A.; Fisher, J.; Weiss, R. *Inorg. Chem.* **1997**, *36*, 4141.
(48) Jian-Fang, M.; Zhong-Sheng, J.; Jian-Zuan, N. *Chin. J. Struct. Chem. (Jiengon Huaxue)* **1996**, *15*, 85.

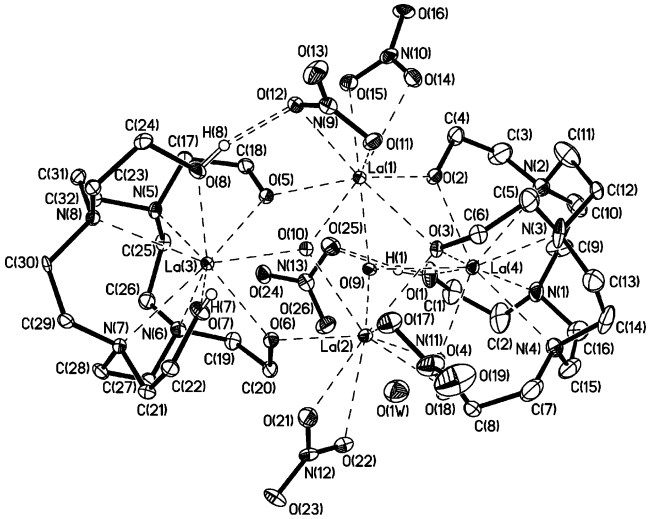

Figure 6. Crystal structure of $[(La(H_2\mathbf{L^1})\{La(NO_3)_2(\mu_3\text{-}OH)\}_2(La(H\mathbf{L^1}))]\cdot(NO_3)\cdot(H_2O)$ (**5**).

abilities of the perchlorate anion), which apparently negate the formation of these clusters.

Structural Description of Polynuclear Complexes of $H_4\mathbf{L^1}$. Structure of $[(La(H_2\mathbf{L^1}))\{La(NO_3)_2(\mu_3\text{-}OH)\}_2(La(H\mathbf{L^1}))]\cdot(NO_3)\cdot(H_2O)$ (5). The crystal structure of $[(La(\mu_3\text{-}(H_2\mathbf{L^1}))\{La(NO_3)_2\}_2(La(\mu_3\text{-}(H\mathbf{L^1})))(\mu_3\text{-}OH)_2(NO_3)]\cdot H_2O$ (**5**) (Figure 6) shows the asymmetric tetranuclear complex to be essentially assembled from one $[La(H_2\mathbf{L^1})]^+$ and two $[La(NO_3)_2]^+$ cations, molecule $[La(H\mathbf{L^1})]$, and one NO_3^- and two bridging $[\mu_3\text{-}OH]^-$ anions. The $[La(NO_3)_2]^+$ species are themselves bridged by the two $[\mu_3\text{-}OH]^-$ groups at O(9) and O(10) and the alkoxide site, O(3). Bridges to $[La(H_2\mathbf{L^1})]^+$ (La(3)) are facilitated by $[\mu_3\text{-}OH]^-$ site O(10) along with alkoxide sites O(5) for La(1) and O(6) for La(2). Bridges to $[La(H\mathbf{L^1})]$ (La(4)) are through the hydroxide O(9) and alkoxide O(3) along with alkoxide sites O(2) for La(1) and O(4) for La(2). The protonated alkoxy sites O(1), O(7), and O(8) do not bridge within the asymmetric unit, but the protons on O(1) and O(8) are involved in stabilizing hydrogen bonding interactions (O(1)−H(1)···O(25) and O(8)−H(8)···O(12)) with nitrate oxygen atoms. The tetranuclear core forms a rare scooplike motif (Figure 7); tetranuclear Ln^{III} clusters are usually in tetrahedral, rectangular, or square motifs.[44] The ligating atoms in the 9-fold coordination polyhedra at La(1) and La(2) are distorted monocapped square antiprismatic, while those at La(3) and La(4) are distorted monocapped square prismatic (Figure 7). The chelate stereochemistry at both $[La(H\mathbf{L^1})]^+$ and $[La(H\mathbf{L^1})]$ is $\Lambda(\lambda\lambda\lambda\lambda)$. The tetranuclear cluster has a maximum diameter (C(30)···C(16)) of ca. 1.36 nm and is therefore a small nanocluster. Intramolecular La···La distances are given in Table 2 and are comparable to other La−O−La links.[49]

Crystal Structures of $[\{Nd(NO_3)_2\}_3(Nd(\mathbf{L^1}))_2(\mu_5\text{-}OH)]$ (6). The gross structures (Figure 8) of the $[\{Nd(NO_3)_2\}_3(Nd(\mu_4\text{-}\mathbf{L^1}))_2(\mu_5\text{-}OH)]$ complex from the room (293 K) and low (110 K) temperature determinations are essentially identical, but the estimated standard deviations of the bond lengths are significantly better for the low temperature study (Table 2) and have been used for quantitative comparative

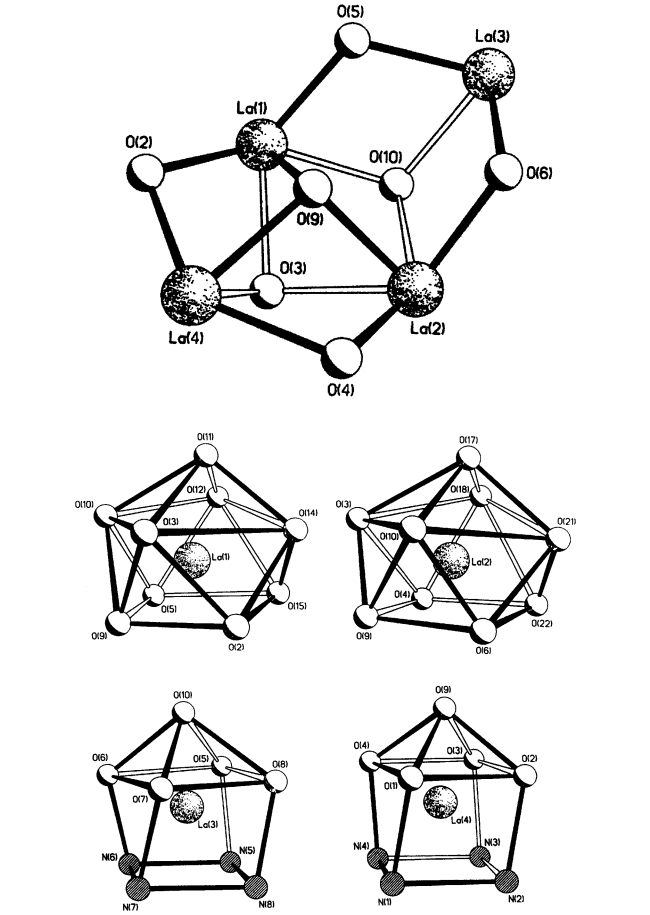

Figure 7. Rare scooplike motif of the La^{III} ions in **5** (top) and coordination polyhedra around corresponding La^{3+} cations.

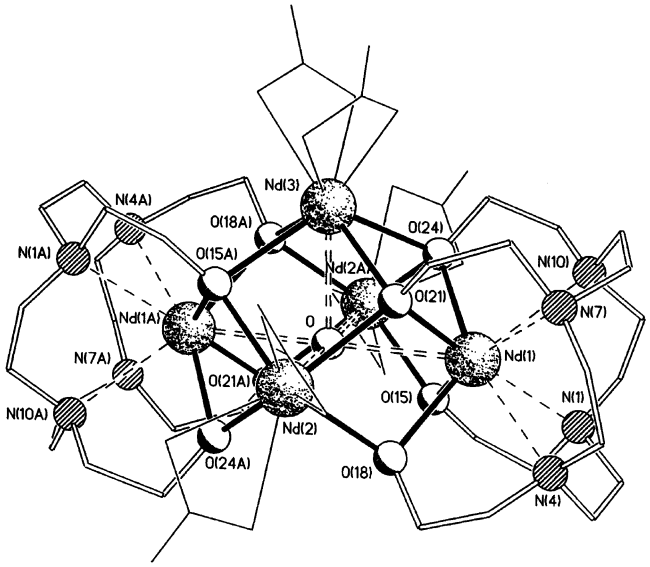

Figure 8. Molecular structure of $[\{Nd(NO_3)_2\}_3(Nd(\mathbf{L^1}))_2(\mu_5\text{-}OH)]$ (**6**). For clarity, the NO_3^- anions are shown as thin lines linked to Nd(2), Nd(2A), and Nd(3). The low and room temperature structures are essentially identical; the room temperature structure is shown.

(49) Barnhart, D. M.; Clark D. L.; Gordon, J. C.; Huffmann, J. C.; Watkin, T. G.; Zwick, B. D. *J. Am. Chem. Soc.* **1993**, *115*, 8461. Mindral, V. F.; Erman, L. Ya.; Gal'perin, E. L.; Kurochkin, V. K.; Petrunin, V. A. *Koord. Khim.* **1991**, *17*, 1290. Hedinger, R.; Ghisletta, M.; Hegetscweiler, K.; Troth, E.; Merbach, A. E.; Sessoli, R.; Gatteschi, D.; Gramlich, V. *Inorg. Chem.* **1998**, *37*, 6698.

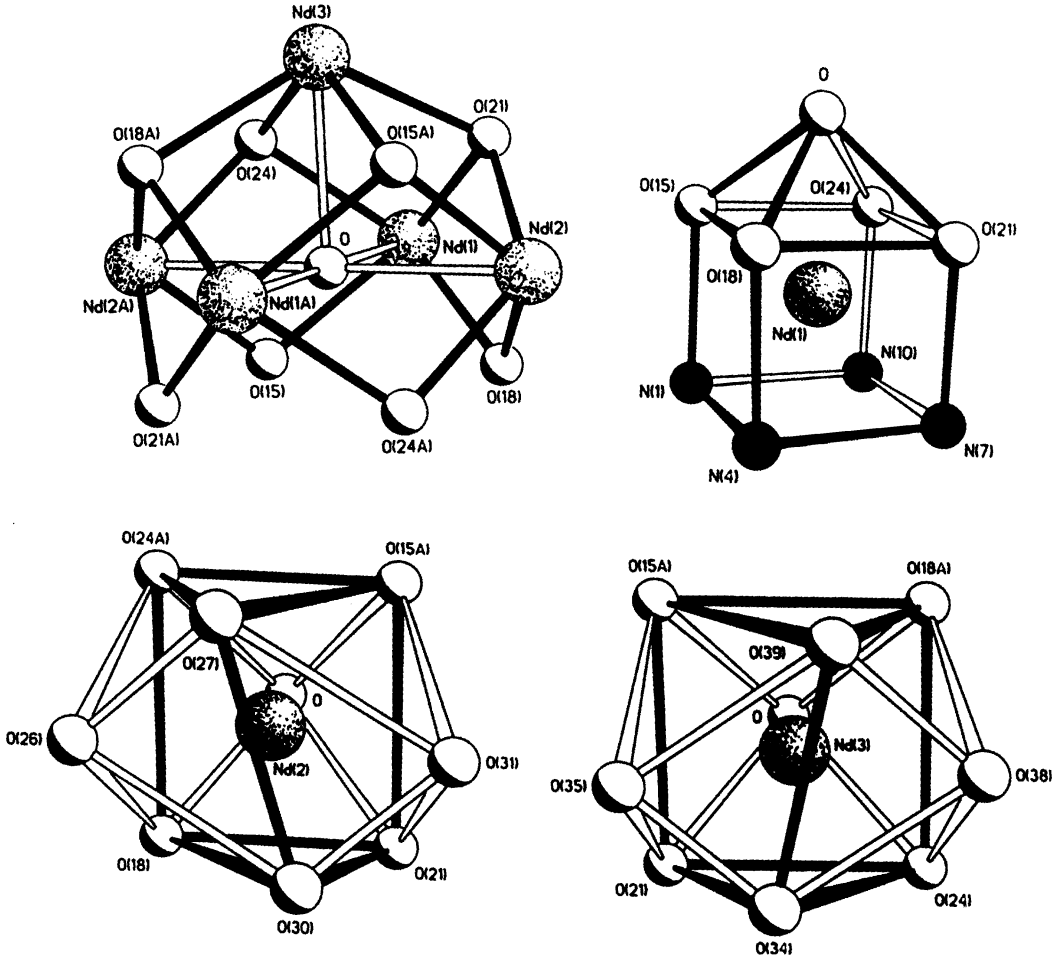

Figure 9. C_{4v} arrangement of the five Nd^{III} ions in **6** (top left). Others: Corresponding coordination polyhedra of Nd atoms.

purposes. The complex is built from two $[Nd(\mu_4\text{-}\mathbf{L^1})]^-$ anions, three $[Nd(NO_3)_2]^+$ cations, and the $[\mu_5\text{-}OH]^-$ anion which "glues" the five cations together to form a square pyramidal C_{4v} arrangement of the Nd^{III} ions (Figure 9). All alkoxide sites are bridging (Figure 8); O(15A), O(18A), O(21), and O(24) are μ_3-OR bridges while O(21A), O(24A), O(15), and O(18) are μ_2-OR. Intramolecular Nd···Nd links across linear Nd−O−Nd bridges (Nd(1)···Nd(1A) and Nd(2)···Nd(2A) (Figure 8)) at 5.51 Å are significantly longer than the literature values of 4.2−5.3 Å.[50] On the other hand, intramolecular Nd···Nd links across bent multiple Nd−O−Nd bridges fall within the range 3.660(1) Å (Nd(2)···Nd(3)) to 3.783(1) Å (Nd(1)···Nd(3)) (Table 2), which is shorter than the 3.76−4.24 Å range reported for such links.[51] The shortest intermolecular Nd···Nd contact is 9.33 Å. The Nd(3) site is disordered (50:50) above (Nd(3)) and below (Nd(3)′) the OH^- anion. Chelate $[\mu_4\text{-}\mathbf{L^1}]^{4-}$ in both $[Nd(\mu_4\text{-}\mathbf{L^1})]^-$ ions features the $\Lambda(\lambda\lambda\lambda\lambda)$ stereochemistry (Supporting Information Figure 3S). The 9-fold coordination polyhedra around the Nd(1) and Nd(1A) are slightly distorted monocapped square prismatic with ca. C_{4v} symmetry (Figure 9); coordination polyhedra at Nd(2) and Nd(3) are distorted trigonal prismatic (Figure 9). The considerably greater distortions in the coordination polyhedra of the dissimilar La**H**$\mathbf{L^1}$ and $[LaH_2\mathbf{L^1}]^+$ species of cluster **5** (Figure 7), compared to those of $[Nd\mathbf{L^1}]^-$ in **6** (Figure 9), might be important and indicative of the distortions required to make clustering possible. The pentanuclear cluster has a maximum diameter (C(16)···C(16)# distance) of ca. 1.20 nm and is a smaller nanocluster than the tetranuclear cluster.

Mass Spectrometry Studies on $[\{Ln(NO_3)_2\}_3(Ln(L^1))_2(\mu_5\text{-}OH)]$. The pentanuclear clusters were characterized by elemental analyses, liquid secondary ion mass spectrometry (LSIMS), and FAB MS studies. The mass spectrometry studies were particularly insightful and indicate almost identical fragmentation patterns for the pentanuclear clusters of Ln^{III} ions across the series, reflecting the homogeneity in composition. Figure 10 shows the LSIMS spectrum of $[\{Y(NO_3)_2\}_3(Y(\mathbf{L^1}))_2(\mu_5\text{-}OH)]$ and indicates the presence of penta-, tetra-, tri-, di-, and mononuclear fragments. The pentanuclear nanocluster $[\{Ln(NO_3)_2\}_3((\mu_4\text{-}\mathbf{L^1}))_2(\mu_5\text{-}OH)]$ generally fragments by losing two NO_3^- anions and H^+ of the OH^- anion resulting in the formation of $[\{Ln(NO_3)_2\}_2$-

(50) Wetzel, T. G.; Roesky, P. W. *Z. Anorg. Allg. Chem.* **1999**, 625, 1953. Igonin, V. A.; Lindeman, S. V.; Struchkov, Yu. T.; Molodtsova, P.; Shchegolinkhina, O. I.; Zhdanov, A. A. *Izv. Akad. Nauk SSSR, Ser. Khim.* **1993**, 193.

(51) Barnhart, D. M.; Clark, D. C.; Huffman, J. C.; Vincent, R. L.; Watkin, J. G. *Inorg. Chem.* **1993**, *32*, 4077. Anderson, R. A.; Templeton, D. H.; Zalkin, A. *Inorg. Chem.* **1978**, *17*, 1961. Ma, W.-W.; Wu, Z.-Z.; Cai, R.-F.; Huang, Z.-E. Sun, J. *Polyhedron* **1997**, *16*, 3723. Herrman, W. A.; Anwander, R.; Scherer, W. *Chem. Ber.* **1993**, *126*, 1533. Decon, G. B.; Feng, T.; Hockless, D. C. R.; Junk, P. C.; Skelton, B. W.; White, A. H. *Chem. Commun.* **1997**, 342. Li, F.; Jin, Y.; Song, C.; Lin, Y.; Pei, F.; Wang, F.; Hu, N. *Appl. Organomet. Chem.* **1996**, *10*, 761.

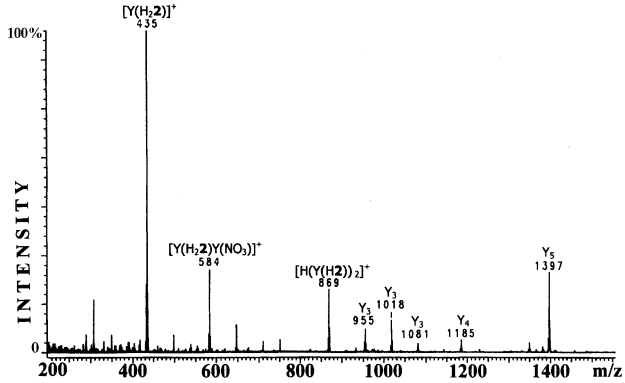

Figure 10. LSIMS of $[\{Y(NO_3)_2\}_3(Y(\mathbf{L^1}))_2(\mu_5\text{-OH})]$ $\{Y_5 = [(Y(NO_3)_2)_2(YO)(Y\mathbf{L^1})_2]^+$ (calcd $m/z = 1397$), $Y_4 = [(Y(NO_3)_2)_2(HO)(Y\mathbf{L^1})_2]^+$ (calcd $m/z = 1185$), $Y_3 = [(Y(NO_3)_2)(YH\mathbf{L^1})_2]^+$ (calcd $m/z = 1081$), $[(Y(NO_3)H(Y\mathbf{L^1})_2]^+$ (calcd $m/z = 1018$), and $[Y(Y\mathbf{L^1})_2)]^+$ (calcd $m/z = 955$)$\}$.

Table 3. Fragments Observed in MS of $[\{Ln(NO_3)_2\}_3(Ln\mathbf{L^1})_2(\mu_5\text{-OH})]$ $\{Ln = Pr-Ho, Y\}$

fragment	Pr	Nd	Eu	Ho	Y
$[\{Ln(NO_3)_2\}_2Ln(OH)(Ln\mathbf{L^1})_2]^{2+}$			857		
$[\{Ln(NO_3)_2\}_2Ln(O)(Ln\mathbf{L^1})_2]^+$	1657			1778	1397
$[(LnNO_3)_2(OH)(Ln\mathbf{L^1})_2]^+$	1393	1404	1437	1490	1185
$[Ln(NO_3)_2(LnH\mathbf{L^1})_2]^+$	1237	1248			1081
$[HLn(NO_3)(Ln\mathbf{L^1})_2]^+$		1183	1206		1018
$[Ln(Ln\mathbf{L^1})_2]^+$		1119	1143		955
$[H(LnH\mathbf{L^1})_2]^+$			994	1021	869
$[Ln_2H_2\mathbf{L^1}(NO_3)_3]^+$	816				
$[(LnH_2\mathbf{L^1})_2(OH)]^+$					584
$[LnH_3\mathbf{L^1}(NO_3)]^+$	549		561		498
$[LnH_2\mathbf{L^1}]^+$	486	488	498	511	435
$[Ln(OH)]^+$		160	170		
$[H(H_4\mathbf{L^1})_2]^+$		697			
$[H(H_4\mathbf{L^1})]^+$		349		349	349

$Ln(\mu_5\text{-O})(Ln(\mathbf{L^1}))_2]^+$. Further fragmentation proceeds by loss of a $Ln(NO_3)_2$ moiety resulting in the formation of tetranuclear $[(Ln(NO_3)_2(OH)(Ln(\mathbf{L^1}))_2]^+$ clusters. Subsequent fragmentations result in the formation of tri-, di-, and mononuclear fragments of varying stoichiometries as shown in Table 3. The complete mass spectral results for pentanuclear clusters of Pr^{III}, Nd^{III}, Eu^{III}, Ho^{III}, and Y^{III} are summarized in Table 3. An interesting feature of the mass spectra is the formation of the $[(LnH\mathbf{L^1})_2]$ dimer, which results from fragmentation and reassembly of the $[Ln(\mathbf{L^1})]^-$ anions. This high-energy process indicates that the formation of such a molecule in solution may be practical. Indeed, we have observed this with Gd, Er, and Yb (confirmed by FAB MS and elemental analyses), but definitive crystallographic structural evidence is lacking.

Ethylenediamine-Terminated Ring-Opening Self-Amination of 1-Aziridineethanol and Resulting Ln^{III} Complexes of H_2L^2. The primary role of ethylenediamine ($pK_a = 7.6$ and 10.7) in the Ln^{III} reactions with 1-aziridineethanol is as a base, facilitating proton abstraction from $H_4\mathbf{L^1}$ ($pK_a = 7-7.5$). However, the products formed from a reaction involving 1-aziridineethanol, praseodymium(III) nitrate, and ethylenediamine revealed the presence of Pr^{III} complexes of $H_2\mathbf{L^2}$, the first member ($n = 1$) of series B. The insoluble Pr^{III} complex formed at high dilution (**7**) is intractable. However, the FAB MS (Supporting Information Figure 4S) is dominated by a peak at $m/z = 235$ which we assign to

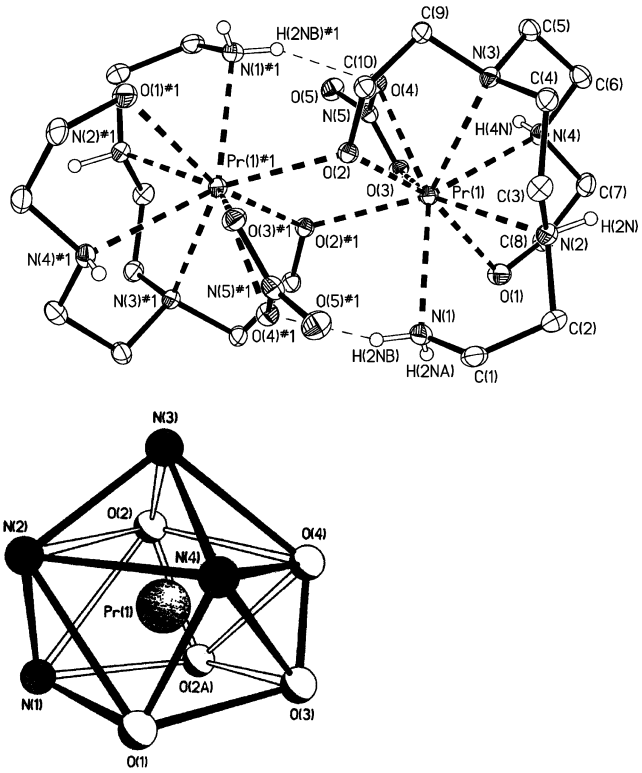

Figure 11. Molecular structure of the $[Pr(\mathbf{L^2})(NO_3)]_2$ dimer (**8**) and the coordination polyhedron around the corresponding Pr^{III} ions (bottom).

$[H_3\mathbf{L^2}]^+$; the other peaks at $m/z = 373$ and 436 are assigned to $[Pr(\mathbf{L^2})]^+$ and $[Pr(H\mathbf{L^2})(NO_3)]^+$, respectively. Slow evaporation of the filtrate yielded small quantities (4% yield) of green crystals of stoichiometry $[Pr(\mathbf{L^2})NO_3)]_2 \cdot HNO_3 \cdot 3H_2O$ (**8**). The FAB MS of the paste (**9**) left after complete evaporation of the solvent from the filtrate (Supporting Information Figure 5S) also revealed the presence of $H_2\mathbf{L^2}$ and its Pr^{III} complexes {namely $m/z = 373$ ($[Pr(\mathbf{L^2})]^+$), 436 ($[Pr(H\mathbf{L^2})(NO_3)]^+$), 499 ($[Pr(H_2\mathbf{L^2})(NO_3)_2]^+$}. No other members of series A and B or their Pr^{III} complexes were observed in the FAB MS.

The identity of the green crystalline product was conclusively established by single crystal X-ray diffraction as $[Pr(\mathbf{L^2})(NO_3)]_2 \cdot$solvent (**8**) (Figure 11-top), which is a praseodymium(III) dimeric complex of the novel poly(amino-alkoxide) chelate $[\mathbf{L^2}]^-$. Because of unresolved disorder in the solvent regions (not near the coordination sphere of Pr^{3+}), only the well characterized dimer $[Pr(\mathbf{L^2})(NO_3)]_2$ is herein discussed.

The Pr^{III} ions are in a 9-fold coordination polyhedron derived from the four amine and two alkoxide sites of $[\mathbf{L^2}]^{2-}$, a bidentate nitrate anion, and a bridging alkoxide site (O(2)) (which facilitates the dimeric structure). A pair of bridging alkoxide sites (O(2) and O(2)#1) facilitates the dimeric structure which is further stabilized by a pair of N−H···O bonds involving sites N(1) (or N(1)#1) on one molecule and O(4) (or O(4)#1) of the other. The coordination polyhedron around Pr^{III} ions is a slightly distorted monocapped square antiprism (Figure 11, bottom), and the intramolecular Pr···Pr contact is 3.9485(4) Å, which is normal for similar Ln−O−Ln links (3.7−5.5 Å).[52]

The formation of Pr^{III} complexes of the tetraaza member of acyclic series B ($H_2\mathbf{L^2}$) occurs in low yields and is rather enigmatic. Clearly, the formation of [Ln($H_4\mathbf{L^1}$)] is a higher yield competing reaction and appears to be more thermodynamically feasible. $[\mathbf{L^1}]^{4-}$ is octadentate and has four basic O^- donors compared with the two possessed by hexadentate $[\mathbf{L^2}]^{2-}$ and is therefore expected to form more stable Ln^{III} complexes. Nevertheless, the most important revelation of this experiment is that a novel acyclic chelate of series B can be prepared and isolated using Ln^{III} ions. Another method of synthesizing $H_2\mathbf{L^2}$ by traditional organic synthetic protocols would arguably be quite challenging. Further studies toward a better understanding and improvements in preparative conditions of members of series B as well as the influence of other metal ions and primary amines are in progress.

Concluding Remarks

The ring-opening reactions of 1-aziridineethanol as a route to two diverse classes of cyclic and novel acyclic poly(amino-alkoxide) chelates have been demonstrated. The cyclooligomerization of 1-aziridineethanol to form cyclic series A competes favorably with the ethylenediamine-terminated process which produces acyclic series B. Chelates $H_4\mathbf{L^1}$ and $H_2\mathbf{L^2}$, the complexes of which were isolated and studied in detail here, may just be the tip of the iceberg in terms of the variety of cyclic and acyclic chelates that might be isolated from carefully controlled ring-opening self-aminations of 1-aziridineethanol. $H_4\mathbf{L^1}$, in particular, is of biomedical relevance due to the catalytic activity of its Ln^{III} complexes in RNA cleavage[15−21] and interest in such Gd^{III} complexes as contrast agents in MRI.[1]

The role of ligand coordinative unsaturation in the aggregation of Ln^{III} ions to form nanoclusters was illustrated in the syntheses of mononuclear and polynuclear complexes of $[H_x\mathbf{L^1}]^{x-4}$ ($x \leq 4$). Unlike the deprotonated alkoxy groups, protonated alcohol groups of the macrocyclic chelate which are coordinated to Ln^{3+} ions are coordinatively saturated and as such are poor bridges for lanthanide(III) ions in the aggregation process (Figure 6). This is likely to be the case with acyclic $H_2\mathbf{L^2}$ as well, although mononuclear complexes of this chelate were not structurally characterized. Further, while not intuitive, the lanthanide ions in the poly(amino-alkoxide) chelates appear to be coordinatively unsaturated in coordination numbers less than nine. The deprotonated chelates $(\mathbf{L^1})^{4-}$ and $(\mathbf{L^2})^{2-}$ only provide eight and six, respectively, of the nine coordination sites required by the metal ion, which enables the Ln^{3+} ions to bridge to other ligands. This mismatch between the coordination requirements of the metal ion and the denticity of the ligand as well as the availability of coordinatively unsaturated ligand sites is a key to aggregation.

The role of Ln^{III} Lewis acidity in the aggregation process was also highlighted in the syntheses of the tetranuclear and pentanuclear nanoclusters, where the harder Lewis acids (Nd^{III}−Ho^{III}, Y^{III}) relatively easily displace all the protons of $H_4\mathbf{L^1}$ while the relatively softer La^{III} and (to a lesser extent) Pr^{III} ions have difficulty doing so. The crucial role of OH^- ions as "molecular glues", which are important for the aggregation of metal ions to form clusters, has also been demonstrated.

In conclusion, this report has highlighted two design strategies that can be utilized for the syntheses of discrete Ln^{III} clusters, both hinging on the coordinative unsaturation phenomena. Sequential deprotonation of oxygen donors of a multidentate ligand is a valid approach to the manipulation of ligand coordinative saturation leading to aggregation. Another design strategy that has been demonstrated is an incompatibility of ligand denticity with the coordination requirements of the Ln^{III} ion.

The influential role of cooperative effects in the self-assembly process leading to the pentanuclear cluster herein reported and electronic activity among the Ln^{III} ions communicating through common oxygen links are intriguing. A detailed discussion has been published elsewhere and demonstrates the possibility of developing such systems as tunable photonic devices.[37]

Acknowledgment. We thank the Inter-American Development Bank-University of the West Indies (UWI) development program for supporting the UWI work (R&D Project #29) and the UWI for a scholarship to M.K.T. We thank Prof. S. V. Ley and Dr. P. Grice (Cambridge University) and Dr. N. Fender (University of Miami) for assistance with FAB MS and LSIMS.

Supporting Information Available: X-ray crystallographic information and diagrams for the structure determinations of compounds **3**−**6** and **8**; the composition, yields, and elemental analyses of Ln complexes of **6** (Ln = Pr, Nd, Sm − Ho, Y); FAB MS of **1**, **7**, and **9**. This material is available free of charge via the Internet at http://pubs.acs.org.

IC020154A

(52) (a) Wang, S.; Pang, Z.; Smith, K. D. L.; Hua, Y.-S.; Deslippe, C.; Wagner, M. J. *Inorg. Chem.* **1995**, *34*, 908. (b) Cunningham, J. A.; Sievers, R. E. *J. Am. Chem. Soc.* **1975**, *97*, 1586. (c) Hubert-Pfalzgraf, L. G.; Daniele, S.; Bennaceur, A.; Daran, J.-C.; Vaissermann, J. *Polyhedron* **1997**, *16*, 1223.